Available online at www.sciencedirect.com
SCIENCE DIRECT®
Advances in Water Resources 29 (2006) 130–153
Advances in Water Resources
www.elsevier.com/locate/advwatres

# Experimental investigations into processes controlling stream and hyporheic temperatures, Fryxell Basin, Antarctica

Karen Cozzetto [a], Diane McKnight [a,*], Thomas Nylen [b], Andrew Fountain [b]

[a] *Institute for Arctic and Alpine Research, University of Colorado, Boulder, CO 80309, USA*
[b] *Department of Geology, Portland State University, Portland, OR 97207, USA*

Received 11 April 2005; accepted 13 April 2005
Available online 5 July 2005

**Abstract**

Glacial meltwater streams in the McMurdo Dry Valleys, Antarctica exhibit daily cycles in temperature with maxima frequently reaching 10–15 °C, often 10 °C above air temperatures. Hydrologic and biogeochemical processes occurring in these streams and their hyporheic zones strongly influence the flux of water, solutes, and sediment to the ice-covered lakes on the valley bottoms. The purpose of this study was to identify the dominant processes controlling water temperature in these polar desert streams and to investigate in particular the role of hyporheic exchange. In order to do this, we analyzed stream temperature patterns on basin-wide, longitudinal, and reach scales. In the basin-wide study, we examined stream temperature monitoring data for seven streams in the Lake Fryxell Basin. For the longitudinal study, we measured temperatures at seven sites along a 5-km length of Von Guerard Stream.

Maximum temperatures in the Fryxell Basin streams ranged from 8 to 15 °C. Daily temperature changes in the streams averaged 6–9 °C. Stream temperature patterns showed strong diel cycles peaking at roughly the same time throughout the lake basin as well as along the longitudinal gradient of Von Guerard Stream. Further, temperature patterns closely matched the associated net shortwave radiation patterns. Von Guerard Stream experienced its greatest amount of warming, 3–6 °C, in a playa region and cooled below snowfields. Temperatures in several streams around Lake Fryxell converged on similar values for a given day as did temperatures in downstream reaches of Von Guerard Stream not influenced by snowfields suggesting that at a certain point instream warming and cooling processes balance one another. The reach-scale investigation involved conducting two dual-injection conservative tracer experiments at mid-day in a 143-m reach of Von Guerard Stream instrumented with temperature and specific conductance probes. In one experiment, snow was added to the stream to suppress the temperature maximum. Chloride data from monitoring wells installed in the streambed showed that streamwater was infiltrating into the streambed and was reaching the frozen boundary. Temperatures in the hyporheic zone were always cooler than temperatures in the stream. OTIS-P modeling of tracer experiment data indicated that significant hyporheic exchange occurred in both experiments. Reach and cross-sectional heat budgets were established with data obtained from the tracer experiments and from a nearby meteorological station. The budgets showed that net radiation accounted for 99% of the warming taking place in the experimental reach. This result, together with the streams' shallow depths and hence rapid response to meteorological conditions, explains the close linkage between stream temperature and net shortwave radiation patterns. Cross-sectional heat budgets also indicated that evaporation, convection, conduction, and hyporheic exchange contributed to 30%, 25–31%, 19–37%, and 6–21%, respectively, of the non-radiative heat losses in the experimental reach. Thus these processes all worked in conjunction to limit stream temperatures in the Dry Valleys' highly exposed environment. This contrasts with other streams in which convection and conduction may play a warming role. The cooling impact of hyporheic exchange was greater in a losing reach than in a gaining one, and increased hyporheic exchange may have lessened the contribution of conduction to the thermal budgets by decreasing streambed temperature gradients. The cooling contributions of evaporation and convection increased with stream temperature and may thus play a role in constraining stream temperature maxima. Finally, our data indicate that streams act as vectors of

* Corresponding author. Fax: +1 303 492 6388.
*E-mail address:* diane.mcknight@colorado.edu (D. McKnight).

0309-1708/$ - see front matter 
doi:10.1016/j.advwatres.2005.04.012

heat in the Lake Fryxell basin, not only warming the hyporheic zone and eroding the frozen boundary underlying the streams but also accumulating and carrying heat downstream, sending a thermal wave into the lake once a day.


*Keywords:* Stream temperature; Hyporheic zone; Heat budgets; Antarctica; Tracer experiments; Polar desert

## 1. Introduction

Temperature regime is an important characteristic of stream ecosystems, influencing the survival of fish and other aquatic organisms, as well as the solubility of oxygen, and rates of nutrient cycling [2,8]. For these reasons, energy gains and losses that affect stream temperature have been investigated for many years [6,47,48,53]. Energy balances or heat budgets in which the various fluxes are quantified can be used to assess the importance of individual heat budget terms, and such budgets have been successfully used to predict stream temperatures [6,53]. Energy fluxes that take place at the stream surface include radiation, convection, and evaporation or condensation phase changes. Those that take place at the streambed include conduction and friction [55,56]. Incoming streamflow, precipitation, tributary inflows, effluent discharges, groundwater inflow and outflow, evaporative losses, and outgoing streamflow are also energy sources and sinks [55]. Recent heat budget investigations have examined the influence of channel morphology, riparian vegetation, substratum type and other stream characteristics on the heat budgets of streams [31,55]. The components of stream heat budgets vary on both daily and seasonal scales [55–57].

In a recent study of temperate streams in a forested watershed, Story et al. [50] used an energy balance approach to quantify the cooling effect of hyporheic exchange on stream temperature, an energy flux not previously included in heat budgets. The hyporheic zone consists of the area below and adjacent to the stream that exchanges water with the stream. This zone can have a strong impact on the biological, chemical, and physical processes taking place in streams [7,20,49]. Poole and Berman [44] suggested that hyporheic exchange may play an important role as a stream temperature buffer, and Johnson [31] proposed temperature buffering mechanisms. In one scenario, increased hydraulic retention coupled with a large volume of subsurface storage was hypothesized to allow warmer daytime water to mix with cooler nighttime water and thus moderate downstream temperatures [31]. Hyporheic exchange would also increase contact between streamwater and substrates and could enhance conduction from warmer to cooler surfaces [31]. Johnson [31] pointed out that the magnitude of hyporheic influence is related to the proportion of streamwater that flows through the hyporheic zone.

The glacial meltwater streams in the McMurdo Dry Valleys of Antarctica provide a unique hydrologic setting for studying hyporheic exchange processes because many complicating factors, such as terrestrial vegetation, groundwater inflows, and runoff from precipitation, are absent in the cold desert environment [45]. Dry valley streams flow through well-established stream channels [10] for 6–12 weeks during the summer. In these streams, hyporheic zone width is generally two to five times larger than that of the main channel and the depth is constrained by the underlying permafrost, expanding as the active layer thaws during the summer [11]. During the continuous sunlight of summer, these hyporheic zones are ''hotspots'' of biogeochemical processes, providing nutrients for the extensive cyanobacterial mats in the streams and changing the concentrations of major ions as the water flows downstream [22,28,36,39,40]. Although the period of streamflow is limited, hyporheic zone processes are important at the watershed scale because the streams connect the glaciers to closed-basin, permanently ice-covered lakes in the valley floors [4,45].

The purpose of this study was to identify the dominant processes controlling stream temperatures and hyporheic zone thermal gradients in a polar desert glacial meltwater stream and to investigate in particular the role of hyporheic exchange. In this cold environment, stream temperature is a critical characteristic of stream habitat, controlling rates of microbial and biogeochemical processes as well as the thawing of the hyporheic zone [3,10]. Continuous monitoring at stream gauges at stream outlets to the lakes has shown that stream temperatures range from zero to 15 °C during the summer and are often as much as 10 °C higher than air temperatures. As is the case for other low discharge streams in arid, alpine, and clear-cut environments, temperatures can change by as much as 10 °C in a single day [12,13]. The magnitude of daily temperature maxima may influence the rates of instream processes and the overall response of the McMurdo Dry Valleys to climate variability.

## 2. Study site

The McMurdo Dry Valleys region is the largest ice-free polar desert oasis on the coast of Antarctica and is located in the Transantarctic Mountains between

latitudes, 77–78°S and longitude 160–164°E. This region is dominated by barren soils, exposed bedrock, well-established stream channels, permanently ice-covered lakes, and glaciers. The region receives the equivalent of less than 10 cm of water equivalent (WEQ) each year on average in the form of snow [5]. With mean annual air temperatures between −15 and −30 °C [18], as well as a landscape devoid of terrestrial vegetation, the region is an extreme cold desert [33]. Between November and February, during the austral summer, average air temperatures on the valley floor range between −5 and −6 °C. Solar radiation is sufficiently intense for glacier surfaces to generate meltwater, which supplies the streams that flow into the lakes [21]. The glaciers are frozen to their base, and all the flow is from surficial melting [21]. A 1-m active layer of soil thaws above permanently frozen ground, preventing groundwater flow [10].

In Taylor Valley, where the study sites are located, streams vary in length and most of the streams remain first order. Some streams contain abundant microbial mats, and the only riparian vegetation is mosses. Stream characteristics in the Lake Fryxell Basin are summarized in Table 1. Discharge, specific conductance, and temperature of these streams are monitored as part of the McMurdo Dry Valleys Long-Term Ecological Research (MCMLTER) project with measurements recorded at 15-min intervals. The instruments used to make the measurements are listed in Table 2. Because meltwater generation is highly responsive to changes in climate and solar insolation, streamflow is dynamic, with flows varying 5–10 fold over the course of a single day. The timing of diurnal peak streamflows reflects solar position relative to the glacier face and surface [10]. In early October, at the start of the austral summer, snow patches may cover 10% of the valley soils [23], and wind-blown snow often accumulates in patches along stream channels. These patches melt through the summer, however, and in the streams monitored by the MCMLTER, the snow volume is negligible when compared to total annual streamflow. Conovitz [11] showed that the hyporheic zone expands through the summer as the active layer thaws and contracts during the fall as the ground freezes. Hyporheic exchange rates are rapid in dry valley streams compared to other streams [45]. Hyporheic exchange flushes solutes from weathering reactions into the stream [22,24] and influences patterns of nutrient uptake and transformation by stream microbial mats [25,40].

The experiments reported here were conducted in Von Guerard Stream, a 5.2 km stream located on the south side of Fryxell Basin. Von Guerard Stream drains an alpine glacier in the Kukri Hills and flows into the eastern end of Lake Fryxell. The stream flows through

Table 1
Characteristics of streams in the Lake Fryxell Basin

| | Length (km) | Aspect | Time of peak flow |
|---|---|---|---|
| Canada Stream | 1.5 | South | 14:30–16:00 |
| Huey Creek | 2.1 | South | * |
| Lost Seal Stream | 2.2 | South | 18:00–24:00 |
| McKnight Creek | 2.0 | West | * |
| Aiken Creek | 1.3[a] | West | * |
| Von Guerard Stream | 5.2 | North | 20:00–23:00 |
| Harnish Creek | 5.1 | North | * |
| Crescent Stream | 5.6 | North | 19:00–22:00 |
| Delta Stream | 11.2 | North | 21:00–23:00 |
| Green Creek | 1.2 | East | * |

The stream length and time of peak flow information presented in this table is from Conovitz [10].
*Indicates data not available.
[a] The stream length for Aiken Creek is only for the reach between Many Glaciers Pond and Lake Fryxell.

Table 2
Instrumentation and accuracy of measurements

| Parameter | Instrument | Accuracy |
|---|---|---|
| *MCMLTER monitoring data* | | |
| Air temperature | Campbell Scientific 207 temperature/relative humidity probes | <±0.4 °C |
| | Campbell Scientific 107B temperature probes | ±0.2 °C |
| Soil temperature | Campbell Scientific 107B temperature probes | ±0.2 °C |
| Incoming/outgoing shortwave radiation | LI-COR model LI 200X silicon pyranometers | <±5% |
| Stream stage | Paroscientific Corporation PSS-1 or PS-2 pressure transducers together with Sutron Corporation Accubars | ±0.01 (L/s) |
| Water temperature | Campbell Scientific 107B temperature probes | ±0.2 °C |
| *Von Guerard Stream temperature profile* | | |
| Water temperature | Optic StowAway Temp logger | ±0.1 °C |
| | Campbell Scientific 107B temperature probe at the gauge station | ±0.2 °C |
| *Tracer experiments* | | |
| Water temperature | Campbell Scientific 107B temperature probes | ±0.2 °C |
| | Optic StowAway Temp logger | ±0.1 °C |
| Specific conductance/water temperature | Campbell Scientific CS547A conductivity/temperature probe | ±5% (SC)<br>±0.4 °C |

unconsolidated alluvium that has multiple lithologic sources, resulting in hyporheic sediments being comprised of granite, gneiss, dolerite, Beacon sandstone [17,43], and carbonate deposits [27]. The porosity of the hyporheic sediment ranges from 0.29 to 0.47 in Von Guerard Stream [11]. The experimental reach was surveyed by UNAVCO using a global positioning system (GPS) unit in which the GPS antenna was mounted on a backpack and walked down the thalweg of the reach. The data were collected in a post-processing kinematic mode and processed relative to base station less than one kilometer away. The gradient of the reach was found to be 0.026 m/m. Algal mats are abundant in the middle reaches, but are sparse in the upper and lower reaches [1,38].

To obtain simultaneous stream temperature readings for evaluation of longitudinal changes in stream temperature, six Optic StowAway temperature probes were installed on the streambed surface at sites along Von Guerard Stream during January 2004 (Fig. 1). A seventh Campbell Scientific temperature probe was located at a gauge station near the mouth of the stream. In the upper reach, the gradient is steep, and a 20 m wide channel cuts through high, steeply sloping banks covered with snow. The uppermost temperature probe was located in this channel at site A. A second probe at site B was located at the base of this steep reach above a point where the flow divides and moves into a playa area. The flow to the west eventually enters Harnish Stream. The playa reach of Von Guerard Stream was snow-free. In this reach, the banks are low, the stream is braided, and shallow pools are common. A third temperature probe, probe C, was installed at the bottom of the playa. Below the playa the gradient is moderate and the stream has a 10–20 m wide channel with a stone pavement and steep, high banks. Probe D was located in this section. The stream then flows into a large snowfield spread out over 60 m, where probe E was placed. About 1.5 km from the lake outlet, the gradient is shallow and the streambed is sandy. Probe F was installed in this stretch. A seventh temperature probe was located at site G, the gauge station situated at a natural control site about 100 m from the mouth of the stream [52]. This gauge station records water stage and temperature on a 15-min interval and has been in operation since 1990. The peak streamflows at the gauge occur between 20:00 and 23:00 [10].

Stream temperature measurements and tracer experiments were conducted during the main flow period in January 2004. The experimental reach was located

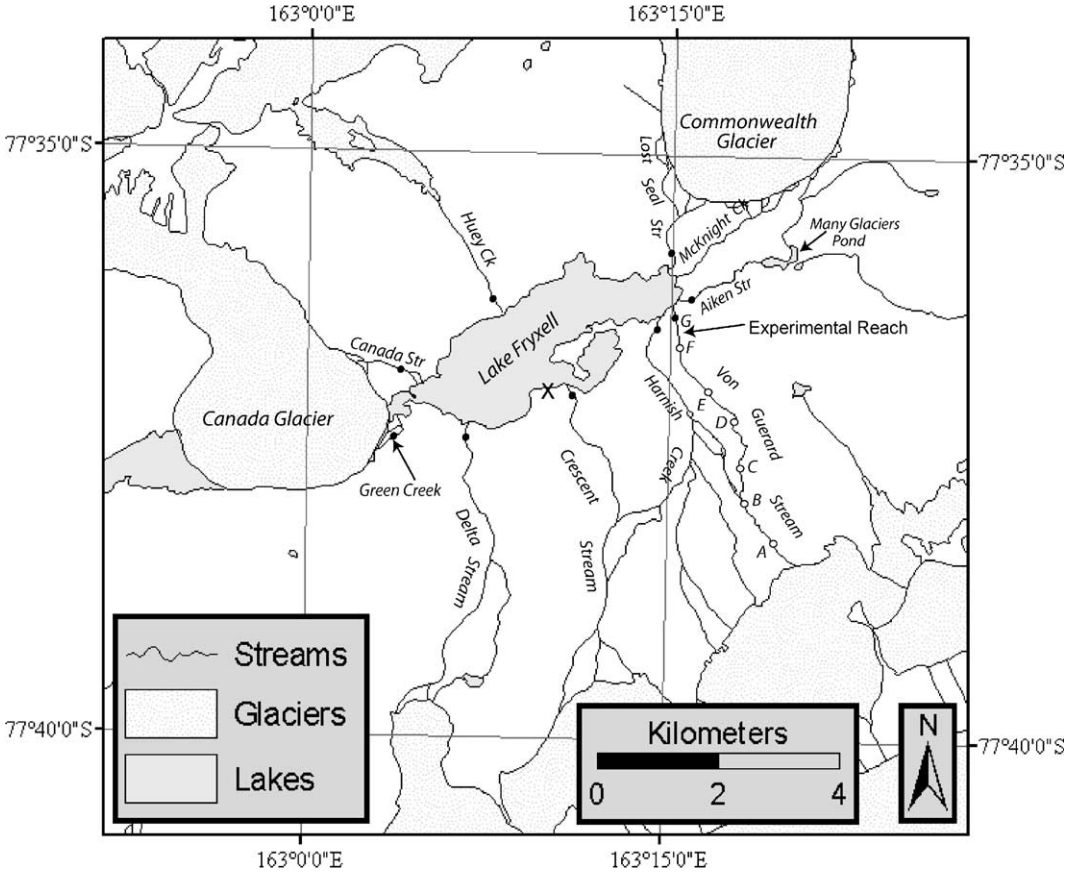


Fig. 1. Lake Fryxell Basin map. Dots represent the location of gauge stations. Open circles represent the location of Optic StowAway temperature probes on Von Guerard Stream. Letters correspond to site descriptions in the text. "X" represents the location of the meteorological station.

187 m below a large snowfield that covered the stream banks on both sides (Fig. 1). We selected an experimental reach where a significant temperature change was expected to occur based on synoptic temperature measurements taken in the reach prior to the experiments. The stream reach also contained a minimum of surficial dead-water areas [34] and microbial mats that could have been disturbed by the sampling activities.

## 3. Methods

### 3.1. Approach

We examined stream temperature patterns on basin-wide, longitudinal, and reach scales. For the basin-wide study, we analyzed existing monitoring data from seven stream gauge stations and one meteorological station in the Lake Fryxell Basin to determine how factors such as stream length, stream aspect, and patterns in net shortwave radiation affected stream temperature. We determined daily and annual temperature ranges and identified maximum temperatures that occurred in the streams. For the longitudinal study, we measured temperatures at seven sites along a 5-km length of Von Guerard Stream to examine the thermal impacts of features such as snowfields and playas. The reach-scale investigation involved studying the influence of hyporheic zone exchange on streamwater temperatures and on thermal gradients in the hyporheic zone. Two conservative tracer injection experiments were conducted in a 143-m reach instrumented with temperature and conductivity probes. In order to examine the impacts of cooler vs. warmer temperature regimes, during one experiment, snow was added to the stream while during the second experiment snow was not added. Reach and cross-sectional heat budgets were constructed from data obtained during the two experiments.

### 3.2. Long-term stream and meteorological station monitoring

The Lake Fryxell Basin analysis was done using data for a typical low flow season, 1997–98, presented on the MCMLTER web site at http://www.mcmlter.org. Meteorological data were from the Lake Fryxell meteorological station, located about 200 m from the experimental reach. Because Lake Fryxell receives relatively uniform amounts of incoming radiation [15], use of the incoming shortwave radiation measured at the meteorological station is a reasonable approximation of the amount of energy received by the experimental reach. In Von Guerard Stream temperature data were obtained using Optic StowAway temperature probes. The probes were installed in areas shaded by instream rocks so that the probes would not be heated directly. Instruments used in the tracer experiments included temperature probes and specific conductance probes. Details of all instruments used in this study and the accuracies of the probes as specified in their operating manuals are presented in Table 2. The Optic StowAway probes were calibrated in an ice bath. All the probes were accurate to within ±0.25 °C and most were accurate to less than ±0.1 °C. Two of the twelve Campbell Scientific 107B temperature probes used were tested by placing them in an ice bath. Both recorded temperatures within ±0.05 °C of 0 °C.

### 3.3. Hyporheic thermal response tracer experiments

Two tracer experiments were conducted over the same reach at approximately the same time of day. We employed a constant-rate dual injection approach with conservative tracers to evaluate the gain and loss of water in the reach. Because the highly variable flows of dry valley streams cause changes in hyporheic exchange, some reaches may gain water from the hyporheic zone at certain times in the diel cycle and lose water at other times.

Previous tracer experiments in the Dry Valleys have shown that the chloride and sulfate behave conservatively [40,45], and these anions were used as injectates. During the snow addition experiment, a 0.336 M solution of NaCl was injected at the top of the reach and a 0.054 M solution of $K_2SO_4$ was injected at the bottom, both at a constant rate of 5 mL/s. During the non-snow addition experiment, 0.079 and 0.022 M solutions of NaCl and $K_2SO_4$ were injected at the top and bottom of the reach, respectively, at a constant rate of 3.33 mL/s. The snow addition experiment injections started at 11:20 and those of the second experiment started at 12:16. The injections for both experiments were stopped at 16:00. The injection points were located at sites with rapid mixing where the stream channel narrowed so that sufficient mixing had occurred above the downstream sampling sites [34].

During the tracer experiments, water samples were collected at several stream sites and monitoring wells and in situ measurements were made of temperature and specific conductance (Fig. 2). Water samples were collected at sites located below the snow addition at 0, 18, 134, and 143 m. The 0 and 18 m samples were above and below the upstream NaCl injection, respectively. The 134 and 143 m sites were above and below the downstream $K_2SO_4$ injection, respectively. At the 0 and 143 m sites, only stream samples were collected. At the 18 and 134 m sites, stream samples as well as samples from two monitoring wells were obtained. The wells were constructed of 2.5-in. PVC pipe following the procedure outlined by Gooseff et al. [24] and were located in the streambed. The two wells were screened at different depths and placed next to one another. The

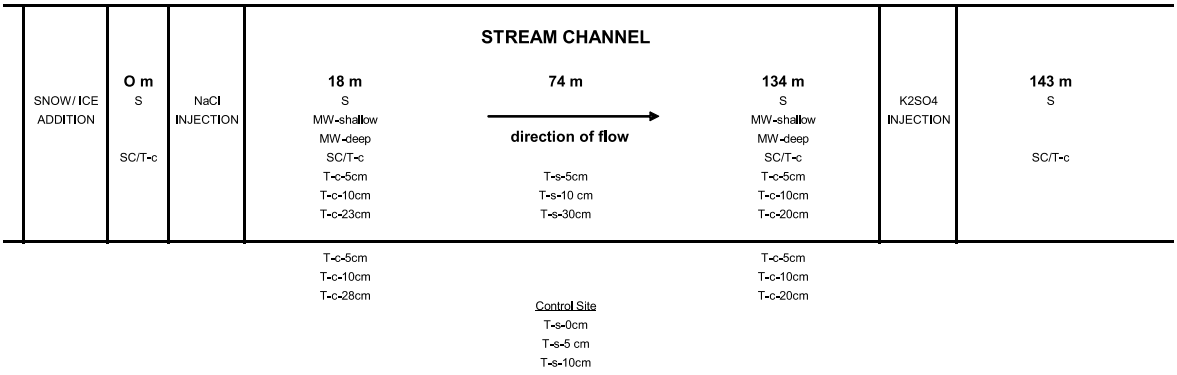


Fig. 2. Schematic of the experimental tracer reach with sampling locations and locations of temperature and specific conductance probes. S = stream sampling location; MW = monitoring well sampling location, SC/T-c = Campbell Scientific CS547A specific conductance and temperature probe; T-c = Campbell Scientific 107B temperature probe at the depth listed; T-s = Optic StowAway temperature probe at the depth listed.

depths screened were 1–11 and 7–17 cm at the 18 m location and 2.5–12.5 and 9–19 cm at the 134 m location.

Stream samples at 0 m, above both injections were collected once per hour to provide background chloride and sulfate concentrations. Stream samples at the 18, 134, and 143 m sites were collected before the injections started and every 5–10 min for one hour after the injections started and ended. At other times stream samples were collected once every 15 min. To take into account possible issues with wells refilling, monitoring wells were sampled once every 30 min. Streamwater samples were filtered on-site using Geopumps and Geotech filter holders equipped with 0.45 μm, 142 mm diameter cellulose nitrate filters. Monitoring well samples were filtered at McMurdo Station using 0.4 μm, 47 mm diameter Whatman Nucleopore filters. All samples were collected in HDPE plastic bottles and were kept chilled, but unfrozen. They were analyzed for chloride and sulfate on a Dionex ion chromatograph at USGS facilities in the Denver Federal Center. The accuracy of the analyses was ±5%.

Stream widths were measured once during each experiment at 10 points along the experimental reach. The measurements were then used to calculate a weighted average width for the stream for use in heat budget calculations and transient storage modeling.

The One-Dimensional Transport with Inflow and Storage model, OTIS-P [45], was used to analyze data from the tracer experiments and obtain values for the longitudinal dispersion coefficient ($D$), the channel cross-sectional area ($A$), the transient storage zone cross-sectional area ($A_s$), and the storage zone exchange coefficient ($\alpha$). Because the reach contained a minimum of surficial dead water areas, it can be assumed that the transient storage in the model represents the hyporheic zone. Flow was assumed to be steady for the two experiments.

Specific conductance measurements were made with Campbell Scientific CS547A probes, which also measured temperature. The probes were placed above and below the injection points in the vicinity of 0, 18, 134, and 143 m. Six Campbell Scientific 107B temperature probes were installed at the 18 m site, three in the streambed at depths of 5, 10, and 23 cm, and three in the hyporheic zone adjacent to the stream at depths of 5, 10, and 28 cm. The 23 and 28 cm deep probes were adjacent to the frozen boundary. Another six temperature probes were set up in parallel fashion at the 134 m site. The depth of the frozen boundary probes in both the streambed and adjacent hyporheic zone was 20 cm (Fig. 2). Optic StowAway probes were also installed in the experimental reach, three in the streambed at 74 m at depths of 5, 10, and 30 cm and three in a nearby dry soil control site at depths of 0, 5, and 10 cm. The Campbell Scientific CS547A specific conductance/temperature probes and 107B temperature probes logged values every minute. The Optic StowAway temperature probes logged values every 15 min.

### 3.4. Heat budget calculations

Heat balances were established for the study reach using data from the two tracer experiments and the Lake Fryxell meteorological station. Story et al. [50] constructed a reach thermal budget that examined the influence of four terms on stream cooling including groundwater, conduction, and hyporheic exchange. Story et al. did not include a friction term in their heat budget. The fourth term grouped together energy fluxes across the water surface. In the thermal budget equation presented below, these terms are separated and the friction term is included. For dry valley streams without tributaries the heat balance can be represented as follows [50]:

$$Q_{\mathrm{us}}T_{\mathrm{us}} + L\beta[H_{\mathrm{radn}} + H_{\mathrm{evap}} + H_{\mathrm{conv}} + H_{\mathrm{cond}} + H_{\mathrm{fr}}] + L[q_{\mathrm{gw}}T_{\mathrm{gw}} + q_{\mathrm{hyp}}(T_{\mathrm{hyp}} - T_{\mathrm{us}})] = Q_{\mathrm{ds}}T_{\mathrm{ds}}$$

$Q_{\mathrm{us}}$ and $Q_{\mathrm{ds}}$ are discharges at the upstream (18 m) and downstream (143 m) boundaries, respectively ($\mathrm{m^3\,s^{-1}}$);

$L$ is the reach length (m); $\beta = w/C$, where $w$ is the average stream width (m) and $C$ is the heat capacity of water ($4.18 \times 10$ J m$^{-3}$ °C$^{-1}$); $H_{radn}$, $H_{evap}$, and $H_{conv}$ are the heat fluxes aross the stream surface due to net radiation, evaporation/condensation, and convection (W m$^{-2}$); $H_{cond}$ is the conductive heat flux across the streambed (W m$^{-2}$); $H_{fr}$ is energy added to the stream from fluid friction (W m$^{-2}$); $T_{us}$, $T_{ds}$, $T_{gw}$, and $T_{hyp}$, are temperatures at the upstream and downstream ends of the reach and of the groundwater and hyporheic zones, respectively (°C); $q_{gw}$ is the loss or gain of groundwater per meter of stream length (m$^2$ s$^{-1}$); and $q_{hyp}$ is the rate at which water exchanges between the stream and the hyporheic zone per meter of stream length (m$^2$ s$^{-1}$). Positive values for $H_{radn}$, $H_{evap}$, $H_{conv}$, $H_{cond}$, $H_{fr}$, $q_{gw}$, and $(T_{hyp} - T_{us})$ indicate heat gain by the stream. Negative values indicate heat loss.

For the snow addition experiment, we established a reach heat budget for each 15-min interval in the experimental period and evaluated the budgets by comparing downstream temperatures predicted using the heat balance with measured temperatures. We did not construct reach heat budgets for the second experiment because the chloride tracer did not reach a plateau. We assessed the influence of terms in the reach heat budgets both in terms of temperature (°C), so that we could compare our results with those of Story et al. [50], and in terms of heat (W m$^{-2}$). As Poole and Berman [44] point out, temperature is proportional to the heat load divided by the discharge and is conceptually a measure of the concentration of heat energy in a stream. Groundwater inflow will add heat to a reach but can decrease the temperature if the groundwater temperature is less than that of the stream.

For the temperature assessment, we used the procedure of Story et al. [50] to determine the contribution of heat budget terms to temperature change for two time periods, one when the stream reach was gaining water and one when the reach was losing water. The cooling or warming effect of conduction ($L\beta[H_{cond}]$), hyporheic exchange $L[q_{hyp}(T_{hyp} - T_{us})]$, and net heat flux across the water surface ($L\beta[H_{radn} + H_{evap} + H_{conv}]$) was determined by calculating the downstream temperature of the reach without the term and subtracting that value from the downstream temperature of the reach as calculated including all four terms. The influence of groundwater was determined by summing the temperature changes attributable to the other three terms and subtracting that value from the total temperature change that occurred between the upstream and downstream ends of the reach.

When assessing the influence of the reach heat budget fluxes in terms of heat, we considered the percent contribution of the terms in W m$^{-2}$ to heat gain or loss in the reach. The terms thus included $H_{radn}$, $H_{evap}$, $H_{conv}$, $H_{cond}$, and $H_{fr}$. We represented hyporheic exchange and groundwater as heat fluxes by averaging their contribution over an area equivalent to the surface area of the reach, $A$, according to: $H_{hyp} = Lq_{hyp}(T_{hyp} - T_{us})C/A$ and $H_{gw} = Lq_{hyp}(T_{gw})C/A$ in which $C$ equals the heat capacity of water. Below we explain how the components of the heat balance equation were determined.

### 3.4.1. Radiation

Incoming shortwave radiation, $SW_{in}$, was measured at the Lake Fryxell meteorological station with a Li-COR pyranometer and recorded at 15-min intervals. Outgoing shortwave radiation over the stream surface was calculated according to $SW_{out} = SW_{in}a$, where $a$ is the albedo of the water surface [16]. Net longwave radiation, $LW_{net}$, was calculated from $LW_{net} = \varepsilon_w\varepsilon_{at}\sigma(T_a + 273.2)^4 - \varepsilon_w\sigma(T_w + 273.2)^4$ in which $LW_{net}$ is in MJ m$^{-2}$ day$^{-1}$, $\varepsilon_w$ is the emissivity of the water surface (0.95), $\varepsilon_{at}$ is the effective emissivity of the atmosphere, $\sigma$ is the Stefan–Boltzmann constant ($4.90 \times 10^{-9}$ MJ m$^{-2}$ day$^{-1}$ K$^{-4}$), $T_a$ is the air temperature in °C as measured at the Lake Fryxell meteorological station, and $T_w$ is the average water surface temperature over the entire reach in °C [16]. The surface water albedo and effective emissivity of the atmosphere were determined according to equations outlined in Dingman [16]. The net radiation flux across the stream surface is thus $H_{radn} = SW_{in} - SW_{out} + LW_{net}$. Because both experiments took place under clear sky conditions and the experimental reach was located in an open area without steep topography, cloud cover and shading effects were not considered.

### 3.4.2. Evaporation

The evaporative heat flux, $H_{evap}$, was calculated using a mass transfer approach, $H_{evap} = LK_EU(e_s - e_a)$ [6,16,50]. $L$, the latent heat of vaporization, and $K_E$, a coefficient that reflects the efficiency of vertical transport of water vapor by the turbulent eddies of the wind were determined from equations outlined in Dingman [16]. $U$, the wind velocity, was measured at the Lake Fryxell meteorological station. The $e_a$ and $e_s$ terms represent the air vapor pressure and the saturation vapor pressure of water, respectively and were determined using data from the meteorological station and equations outlined in Dingman [16].

### 3.4.3. Convection

The transfer of sensible heat between the water surface and overlying air via convection was calculated using the Bowen ratio, $B$, which is the ratio of sensible heat exchange to latent heat exchange. Thus, $H_{conv} = BH_{evap}$. The Bowen ratio is determined according to the equation $B = \gamma(T_w - T_a)/(e_s - e_a)$ in which $\gamma$ is the psychrometric constant calculated as outlined by Dingman [16].

*3.4.4. Conduction*

Conductive heat exchange with the streambed was determined according to $H_{cond} = K(dT/dz)$ in which $K$ is the thermal conductivity of the streambed ($J\ m^{-1}\ s^{-1}\ °C^{-1}$) and $dT/dz$ is the gradient of temperature with depth in the streambed ($°C\ m^{-1}$) [6,31,50,55]. Lapham's graphical relation between dry bulk density and thermal conductivity was used to estimate a streambed $K$ of $2.42\ W\ m^{-1}\ °C^{-1}$ [32]. A dry bulk density of $1.8\ g\ cm^{-3}$ was used based on measurements by Conovitz in a soil core collected near the experimental reach [11]. Other studies used thermal gradients over distances from the streambed surface at 0 cm to a depth of 5 cm, from a depth of 0 to 30 cm, and from a depth of 0–100 cm [31,50,55]. The temperature gradients in the experimental reach were not linear, and we used the 0–10 cm gradient in the calculations.

*3.4.5. Friction*

Energy added to the stream from fluid friction was calculated according to the equation, $H_{fr} = 9805(Q/w)S$ in which $H_{fr}$ is in $W\ m^{-2}$, $Q$ is the average flow in the study reach ($m^3\ s^{-1}$), $w$ is the average width of the stream (m), and $S$ is the slope of the channel [55,56].

*3.4.6. Stream and groundwater discharge and temperature*

Stream discharges at the top and bottom of the reach were obtained from mass balances around the two tracer injection points, and stream temperatures were obtained from in situ measurements.

The net groundwater inflow to or outflow from the stream was calculated from a flow balance by subtracting the upstream flow and water lost to evaporation from the downstream flow. This discharge was then divided by the length of the stream reach to obtain $q_{gw}$, the loss or gain of groundwater per meter of stream length. If the reach was losing water, the groundwater temperature, $T_{gw}$, was set equal to the average water temperature in the reach. If the reach was gaining water, $T_{gw}$ was set equal to the average temperature of the hyporheic zone.

When we discuss groundwater in Taylor Valley we are referring to hyporheic groundwater and not groundwater coming from a watershed aquifer. As Poole and Berman explain, hyporheic groundwater consists of streamwater that enters a stream's alluvium, travels along localized subsurface pathways for relatively short periods of time ranging from a few minutes to several weeks, and then reenters the stream at a downstream location [44]. This is different from groundwater that comes from a watershed aquifer and travels below the surface for much longer time periods and over greater distances than hyporheic water. Taylor Valley does not contain a watershed scale groundwater system [45].

*3.4.7. Hyporheic exchange*

Following Story et al., the storage zone exchange coefficient, $\alpha$, and the channel cross-sectional area, $A$, obtained from the OTIS-P transient storage modeling were used to calculate a hyporheic zone exchange rate according to $q_{hyp} = \alpha A$ [50].

As discussed in the results section, the monitoring well data indicate that streamwater was reaching the frozen boundary. The entire 20–23 cm deep thawed area below the stream was thus considered to be part of the hyporheic zone. We obtained the average hyporheic zone temperatures at the 18 and 134 m locations in the reach by taking the streambed temperatures at the 0, 5, 10, and the 20/23 cm depths and calculating a weighted temperature average over the entire thawed depth for each 15-min interval. It was important to weight the averages because the temperature gradient in the streambed was non-linear. The streambed temperature at 0 cm was assumed to equal streamwater temperature. Temperatures at the other depths were measured in situ.

The cross-sectional thermal budgets considered heat gains and losses in $W\ m^{-2}$ at a particular point and could consequently be constructed for the non-snow addition experiment as well as the snow addition experiment. The cross-sectional budgets included the $H_{radn}$, $H_{evap}$, $H_{conv}$, $H_{cond}$, $H_{fr}$, and $H_{hyp}$ terms of the reach budgets but did not include the term associated with groundwater flow into or out of the stream reach. The $H_{hyp}$ term was calculated according to: $H_{hyp} = q_{hyp}(T_{hyp} - T_{us})C/w$ in which $w$ equals the width of the stream at the point in the reach being considered. Cross-sectional thermal budgets were established for each 15-min interval during the experiments for both the 18 and 143 m locations in the stream reach. Since the reach consistently lost water over the experimental period, the 15-min interval budgets for each location were then averaged to obtain budgets representative of the overall heat losses and gains that took place during the experiments.

## 4. Results

### *4.1. Streamwater temperature variation in Von Guerard Stream and other Fryxell Basin streams*

Maximum temperatures in the seven Fryxell Basin streams whose records were analyzed ranged from 8 to 15 °C, depending on the stream. Because the streams occasionally had minimum temperatures of 0 °C, the seasonal range in temperatures was also 8–15 °C (Table 3). Daily temperature changes in the streams averaged 6–9 °C.

Temperatures in the Fryxell Basin streams peaked at approximately the same time, coincident with the peak

Table 3
Surface water temperature patterns

| Stream type | Maximum temperatures (°C) | Annual temperature range (°C) | Source |
|---|---|---|---|
| Equatorial—southern hemisphere | 13–30 | Generally <5 | [54] |
| Tropical—southern hemisphere | 22–38 | 7–15 | [54] |
| Temperate—southern hemisphere | 6–33 | 0–30 | [54] |
| Glacial streams—high altitude, high latitudes | 10 | – | [41] |
| Arctic | 5–21 | – | [26,29,35,42] |
| Antarctic—Lake Fryxell Basin streams | 8–15 | 8–15 | Current study |

– = Not available.

in solar radiation in the valley (Fig. 3). Further, Aiken Creek, Delta Stream, Von Guerard Stream, Green Creek, and Lost Seal Stream had similar peak temperatures, despite having different orientations and lengths (Table 1). Green Creek occasionally had lower peak stream temperatures. Lost Seal Stream had temperature maxima similar to Aiken, Delta, Von Guerard, and Green, but had colder minimum temperatures.

In Von Guerard Stream, temperatures peaked at about the same time at sites B–G (Fig. 4). The uppermost site A is in shadow at the time of peak solar radiation and temperatures there peaked 1–3 h later.

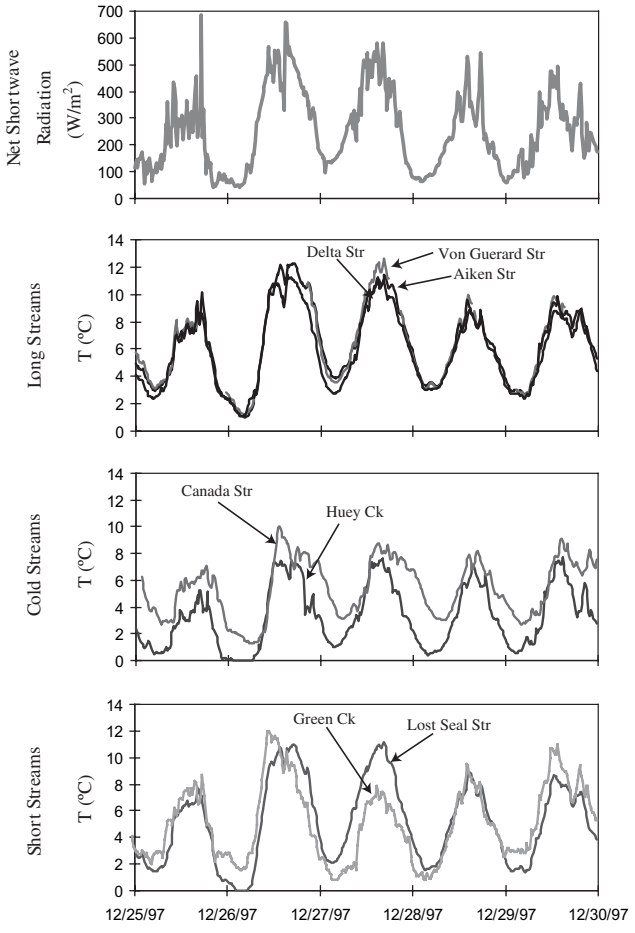


Fig. 3. Water temperatures in seven Lake Fryxell Basin streams for a representative five day period in December 1997.

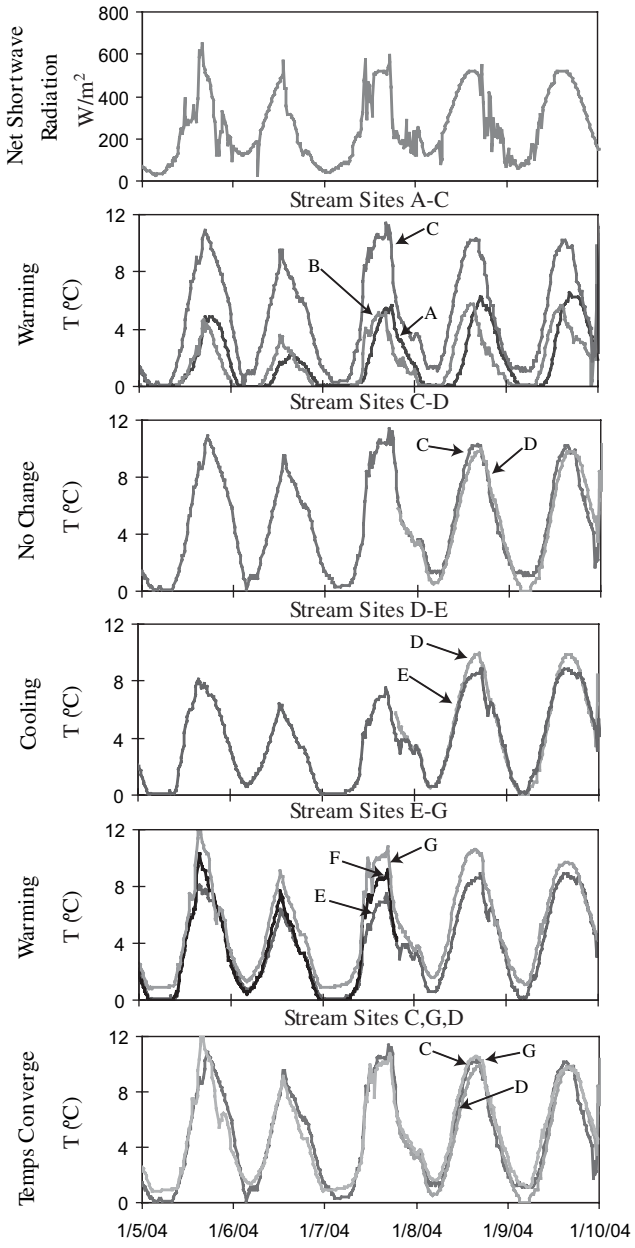


Fig. 4. Longitudinal stream temperature profile along Von Guerard stream for a five day period in January 2004 for seven sites, A–G. Significant channel characteristics are as follow: A—steep gradient, banks covered with snow, B—at the base of steep gradient reach, C—at the base of a playa region, D—moderate gradient, 10–20 m wide, E—in middle of a large snowfield, F—shallow gradient, sandy streambed, G—gauge station 100 m from mouth of stream.

As seen for the other Fryxell Basin streams, maximum temperatures were roughly coincident with the maximum solar radiation. Fig. 4 also illustrates the effect of instream features on longitudinal warming and cooling trends. Warming took place as the stream flowed from the glacier, past sites A and B, to the base of a playa region at site C. The greatest longitudinal increase in temperature occurred in this playa reach, with as much as a 6 °C increase between sites B and C at the time of peak temperatures. There was little temperature change from site C to D, where the streamflows through a more channelized snow-free reach. Between sites D and E, the stream flows through another large snowfield, and the maximum stream temperatures cooled by about 1 °C. Below site E, there were no more large snowfields and the stream temperature increased steadily downstream. At the gauging station (G), peak stream temperatures had almost returned to the high values that occurred in the upper playa reach (C and D).

### 4.2. Hydrologic context of the tracer experiments

The hydrologic and climatic context of tracer experiments is illustrated in Fig. 5. The two experiments occurred under low flow conditions. The days preceding the snow-addition experiment were warmer than those preceding the non-perturbation experiment, which occurred on the first warm day following a cold spell. The air temperatures during the two experiments were comparable, as were the peak net shortwave radiation

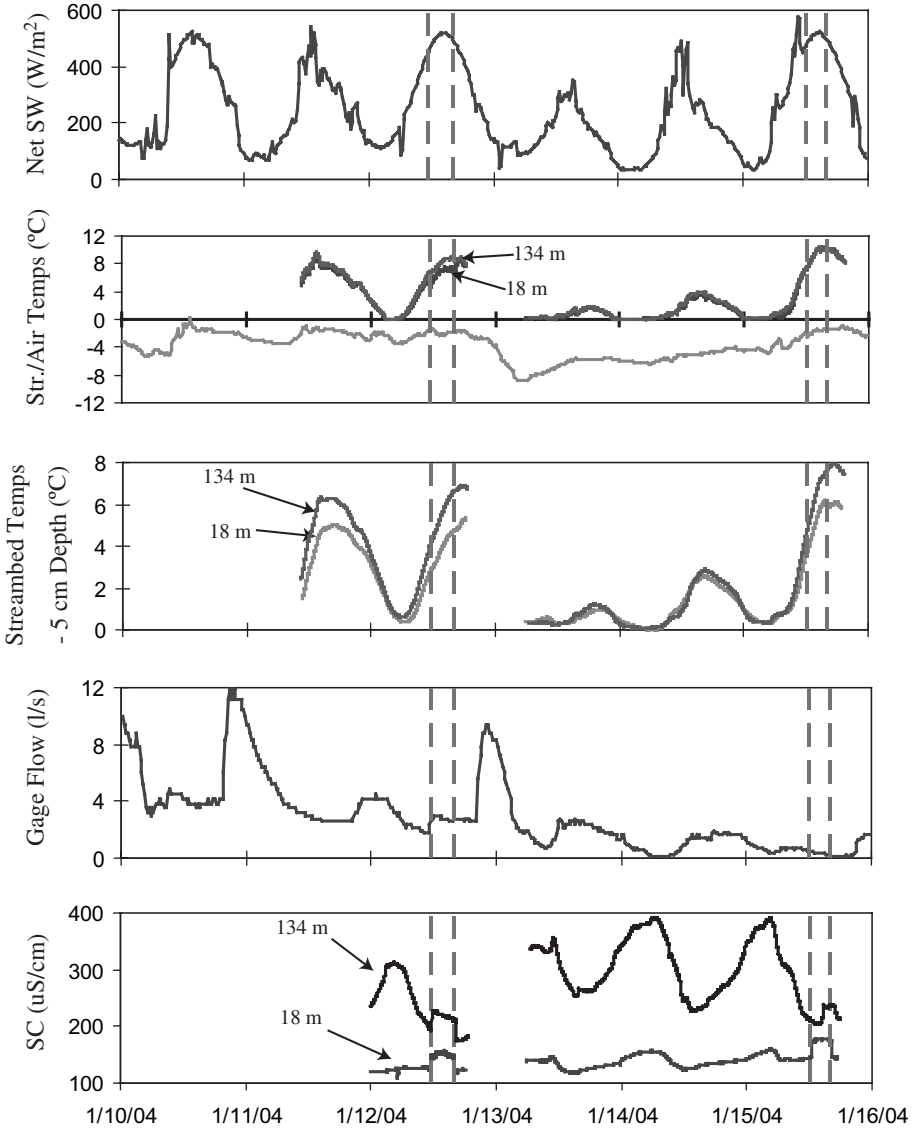


Fig. 5. Net shortwave radiation, streamwater temperature, air temperature, streambed hyporheic zone temperature, and specific conductance data for the experimental reach before, during, and after the tracer experiments. Flow data from a gauge station 638 m downstream of the start of the experimental reach are also presented. The dashed lines indicate the start and end of the tracer injections.

values during the tracer injections. There was a spike in net shortwave radiation prior to the start of the second experiment. However, such spikes sometimes occur when a sensor is hit by a burst of sunlight after a cloud has passed. Net shortwave radiation, stream and hyporheic temperatures, flows, and specific conductance at 134 m all showed a daily cycle. Air temperature and specific conductance at 18 m varied as well, but exhibited less pronounced daily cycles. Peak flows and peak conductance were offset in terms of timing when compared to net shortwave radiation, surface soil, and stream temperatures.

Streamwater temperatures were in some cases 10 °C warmer than air temperatures (Fig. 5). Stream temperatures at the 18 and 134 m sites were fairly close, except during the snow addition which resulted in cooler temperatures at the 18 m site. On the comparatively warm days, the 5 cm streambed temperatures at the 134 m site reached maxima that were 1–2 °C warmer than the corresponding maxima at the 18 m site. The specific conductance values at the 134 m site were 60–70 μS/cm greater than those at the 18 m site during the tracer experiments and were as much as 230 μS/cm greater on some days.

### 4.3. Snow perturbation experiment

During the snow addition experiment, stream temperatures decreased by 1–2 °C from above to below the snowfield (Fig. 6). The snow addition below the snowfield enhanced this decrease by 0.5–1 °C as measured at the 0 and 18 m sites. The snow addition was sufficient to suppress stream temperatures to about 7.5 °C. The stream proceeded to warm by 1–2 °C as it flowed to the 134 m site. However, the temperature at that site did not reach the above-snowfield temperatures. In the short reach between the 134 and 143 m sites the stream temperatures consistently cooled by about 0.5 °C. Temperatures increased with time at the downstream sites. After the snow addition stopped, the temperature at the 0 and 18 m sites was 2 °C greater than before the snow addition began.

During the experiment, chloride concentrations at the 18 m site increased from background levels of 7–8 mg/L to concentrations varying between 14 and 19 mg/L. This

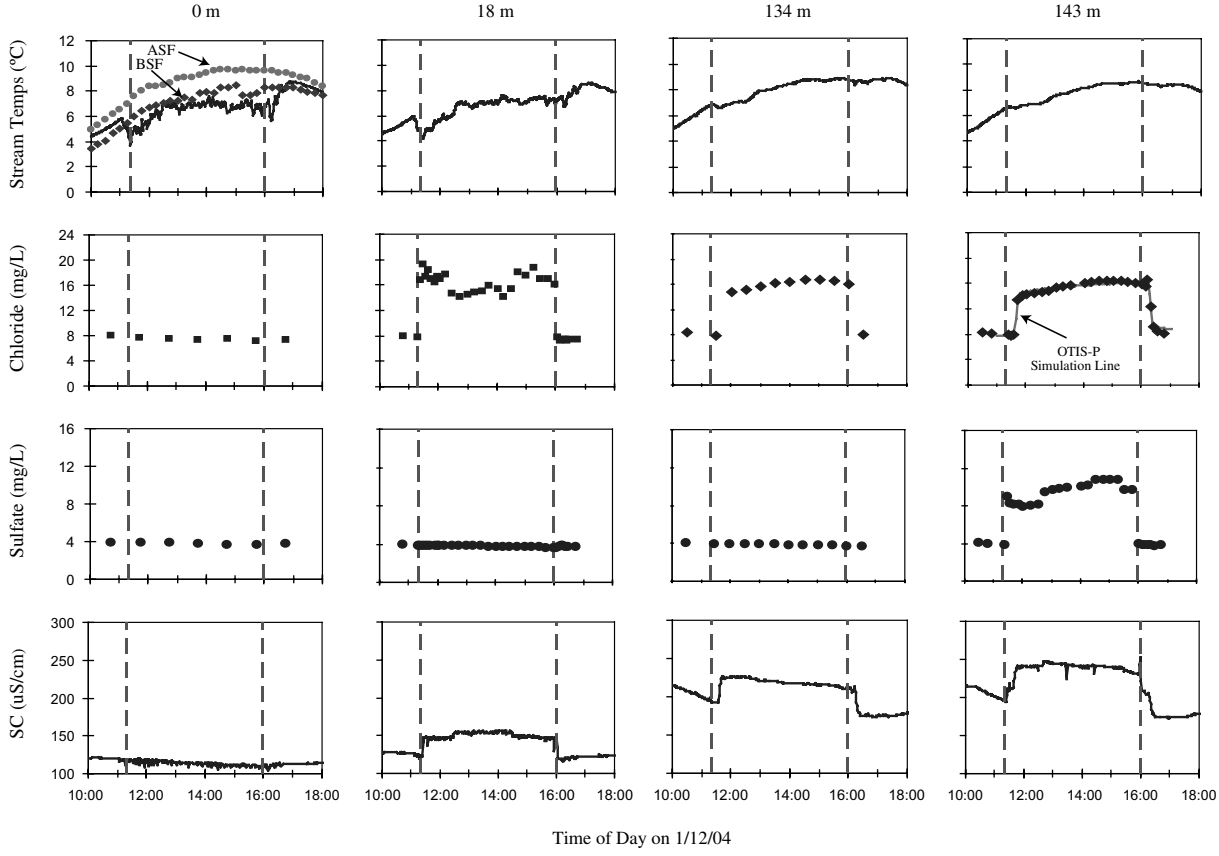


Fig. 6. Results of the snow addition tracer experiment showing changes in stream temperature, chloride concentrations, sulfate concentrations, and specific conductance at 0, 18, 134, and 143 m. ASF = above the snowfield, BSF = below the snowfield. The dashed lines indicate the start and end of the tracer injections. The 143 m chloride concentrations predicted by the OTIS-P transient storage model are plotted alongside the measured concentrations.

variability was attenuated by the 134 m site. The chloride concentrations at the 143 m site were consistently lower by about 0.5 mg/L than at the 134 m site. Sulfate concentrations at the 143 m site increased from background levels of around 4 mg/L to values between 8 and 11 mg/L during the injection. The concentrations were variable, but not as much as the chloride concentrations at the 18 m site. In general, instream sulfate concentrations at the 143 m site showed an increasing trend during the tracer injection, indicating an overall decrease in flow over time.

The sharp rises and falls in specific conductance associated with the beginning and end of tracer injections were recorded by the instream probes, providing a means to estimate travel times. At the start of the experiment, it took water 6, 20, and 26 min to travel from the first injection point at 4 m to the 18, 134, and 143 m sites, respectively. At the end of the experiment, these travel times were 5, 25, and 30 min, respectively. This similarity in travel times throughout the experiment shows that the velocities in the main channel were generally stable. The changes in the initial and final specific conductance values at all sites reflected the overall decreasing trend occurring during the day.

### 4.4. Non-perturbation experiment

During the second, non-perturbation, experiment, stream temperatures decreased by 2–4 °C from above to below the snowfield (Fig. 7). The stream warmed by 2–3 °C as it traveled to the initial sampling point at 0 m and continued to warm by 0.5–0.7 °C, reaching above-snowfield temperatures at the 18 m site. In contrast to the snow addition experiment, between the 18 and 134 m sites there was no discernible change in stream temperature. Finally, the streamwater cooled 1–1.5 °C from the 134 m site to the 143 m site.

During the experiment, stream temperatures at 18 and 134 m reached about 10 °C, which was about 1.5 and 3 °C higher than corresponding values during the snow addition experiment. However, because the initial stream temperatures were lower during this experiment, the overall temperature gain was higher than the maximum value implies. If starting temperatures at 10:00 are considered, then the temperature gains are 2–3.5 °C greater than those in the first.

During the tracer injections, chloride concentrations at the 18 m site increased from background levels around 10 mg/L to between 19 and 21 mg/L. The concentrations

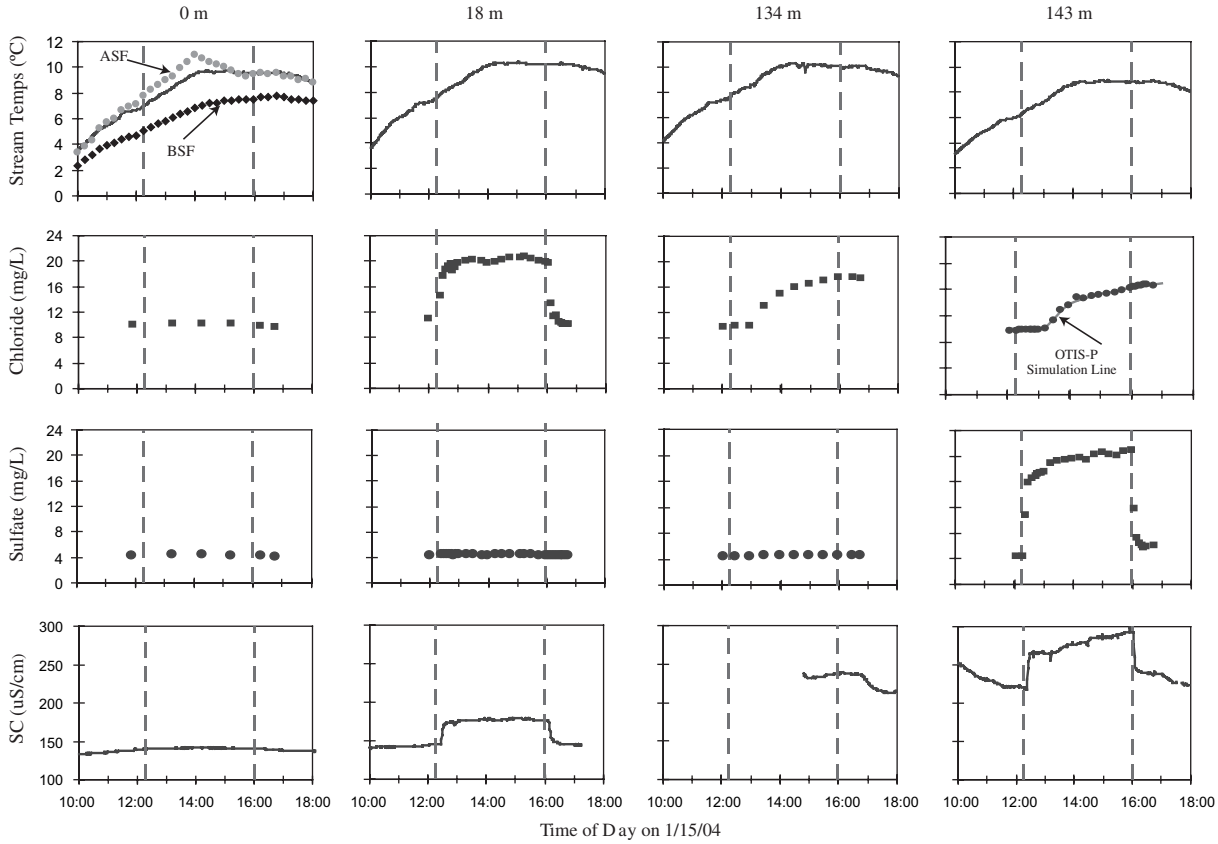


Fig. 7. Results of the non-perturbation tracer experiment showing changes in stream temperature, chloride concentrations, sulfate concentrations, and specific conductance at 0, 18, 134, and 143 m. ASF = above the snowfield, BSF = below the snowfield. The dashed lines indicate the start and end of the tracer injections. The 143 m chloride concentrations predicted by the OTIS-P transient storage model are plotted alongside the measured concentrations.

at 18 m were less variable than during the snow addition experiment. At the 134 m site, chloride concentrations increased gradually and did not reach a plateau until the end of the injections at 16:00, 3.75 h after the injection started. The plateau value was 17.5 mg/L, which was lower than the 18 m concentrations. Between the 134 and 143 m sites, chloride concentrations consistently decreased by about 1.5 mg/L. During the experiment, sulfate concentrations at 143 m initially rose to 16 mg/L and continued to rise to 21 mg/L by the end of the injection, with the rate of change decreasing over time.

The overall travel time through the reach exceeded an hour under the lower flow conditions. Both at the beginning and end of the experiment, travel times from the upstream injection site at 4 m to the 18 and 143 m sites were 18 and 91 min, respectively. During the middle of the experiment, it was discovered that the specific conductance probe at 134 m was only partially submerged, preventing the determination of the initial travel time from 4 to 134 m. The probe was moved to another location at approximately 15:00. The travel time from 4 to 134 m at the end of the experiment was 78 min.

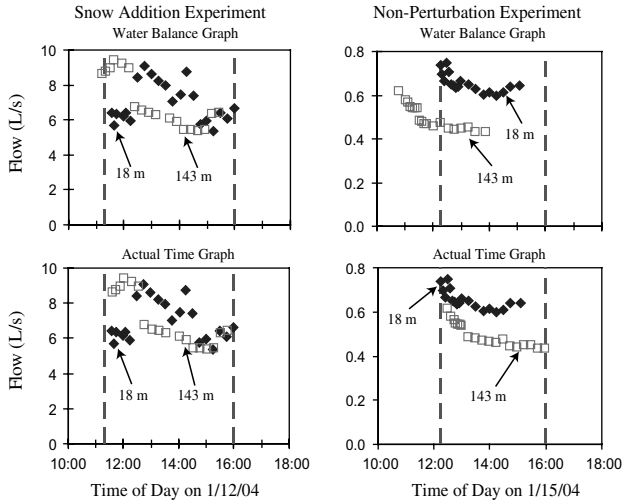


Fig. 8. Calculated flows for the snow addition and non-perturbation experiments. The dashed lines indicate the start and end of the tracer injections. In the water balance graphs, the flows at 143 m have been transposed by the travel time in the reach so that a vertical line between two data points represents a single parcel of water.

### 4.5. Flow regimes and hyporheic exchange during tracer experiments

A mass balance approach based on the known injectate concentrations and flow rates was used to convert the instream chloride concentrations at 18 m and sulfate concentrations at 143 m to streamflow rates. Flows during the snow addition were variable and ranged from 5.4 to 9.4 L/s with changes that were on the order of 0.4–3.5 L/s. Such changes are unlikely to have resulted solely from the snow addition and are comparable to previously measured flow variations in another Lake Fryxell Basin stream [45]. Flows during the second experiment were less variable and were considerably lower, ranging from 0.4 to 0.9 L/s. In Fig. 8, the 143 m flow values are transposed to take into account the travel times between 18 and 143 m, to show the water balance for a particular parcel of water as it traveled through the reach. The thermal budgets take into account the varying flows, and the reach thermal budgets also take into account the time it takes the water to travel from the upstream end of the reach to the downstream end.

The OTIS-P hyporheic zone simulations for the two experiments treated flows in the reach as a steady state by using flow averages. For the snow addition experiment, the inflow rate to the reach was set equal to $0.00702\ m^3\ s^{-1}$ and the lateral inflow and outflow rates were set equal to zero. For the second experiment in which the reach was consistently losing, the inflow rate was set equal to $0.00065\ m^3\ s^{-1}$ and the lateral outflow rate was set equal to $1.47 \times 10^{-6}\ m^3\ s^{-1}$ per meter of stream length. Optimized hyporheic exchange parameters for the simulations are reported in Table 4 along with the associated residual sum of squares. The hyporheic exchange coefficients for both experiments were quite similar, $2.33 \times 10^{-4}$ vs. $2.03 \times 10^{-4}$. However, the cross-sectional hyporheic storage zone cross-sectional area of the snow addition experiment, $0.064\ m^2$, was nearly three times that of the second experiment, $0.024\ m^2$. The 143 m chloride concentrations predicted by the OTIS-P model are plotted alongside measured concentrations in Figs. 6 and 7.

### 4.6. Tracer concentrations in streambed monitoring wells

During the snow addition experiment, the chloride concentrations increased at the wells at the 18 and

Table 4
Transient storage model parameters

| Parameter | Snow addition experiment | Non-snow addition experiment |
|---|---|---|
| $\alpha$, exchange coefficient ($s^{-1}$) | $2.33 \times 10^{-4}$ | $2.03 \times 10^{-4}$ |
| $A$, channel cross-sectional area ($m^2$) | 0.064 | 0.022 |
| $A_s$, storage zone cross-sectional area ($m^2$) | 0.109 | 0.041 |
| $D$, dispersion coefficient ($m^2\ s^{-1}$) | 0.17 | 0.061 |
| RSS, residual sum of squares | 3.97 | 0.83 |

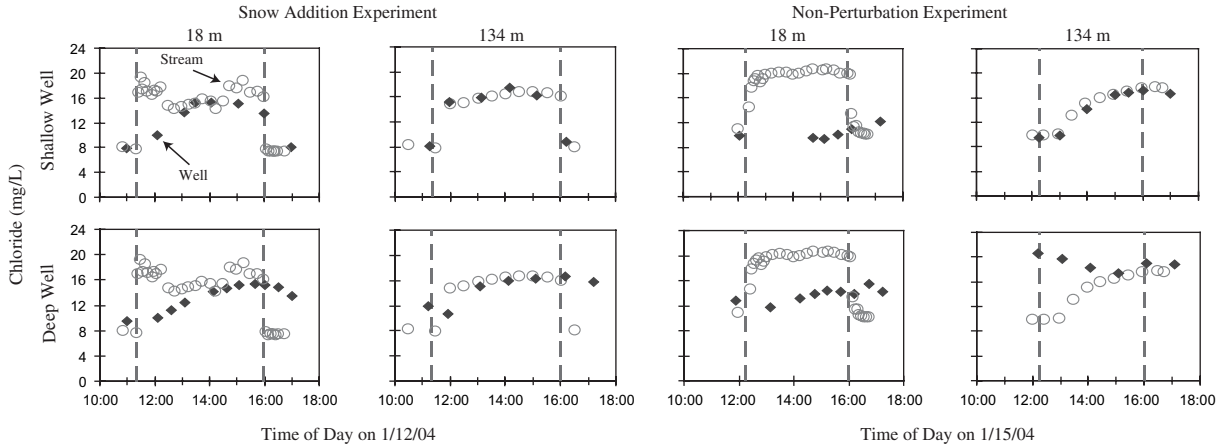


Fig. 9. Chloride concentrations in streambed monitoring wells at 18 and 134 m during the two experiments. Filled in diamonds represent the monitoring well chloride concentrations. Open circles represent the corresponding instream chloride concentrations. The dashed lines indicate the start and end of the tracer injections.

134 m sites (Fig. 9), indicating that streamwater was infiltrating into the hyporheic zone. The chloride increase in the 18 m wells was slower than that in the 134 m wells. The wells did not reach instream concentrations until between 13:30 and 14:00, which indicates a weaker connection between the stream and hyporheic zone at this location. In contrast, in the two wells at 134 m, chloride concentrations rapidly increased to instream values after the injections started and stayed at those levels throughout the experiment indicating a strong hyporheic zone-stream connection.

During the non-snow addition experiment, the chloride levels in the 18 m wells remained far below instream values (Fig. 9) throughout the injections, indicating perhaps even less hyporheic zone water–streamwater exchange at this site than during the previous experiment. In the 134 m shallow well, chloride levels matched instream concentrations throughout the entire injection. The deeper 134 m well initially had chloride concentrations that were much higher than instream values, 20.6 vs. 9.8 mg/L. However, these concentrations decreased during the experiment. This seems to indicate that streamwater was diluting the hyporheic water. By the 15:00 sample, the well and instream concentrations matched. So, as in the snow addition experiment, the 134 m location seemed to have a strong hyporheic zone-stream connection.

Except in one instance, all wells during both experiments had sulfate concentrations that consistently remained at around 4 mg/L, which matched background instream sulfate concentrations. The exception was the deeper well at 134 m during the non-snow addition experiment. In this case sulfate concentrations in the well were slightly higher at 6.5 to 8 mg/L. The well sulfate concentrations are not presented.

### 4.7. Patterns in hyporheic zone temperatures

Fig. 10 shows a longitudinal cross-section of stream and hyporheic temperatures at the 18, 74, and 134 m sites in the experimental reach. During the snow addition streamwater warmed 1–2 °C as it flowed through the reach. The streambed hyporheic zone also exhibited a warming trend from 18 to 134 m, with 5 cm depths showing a 1–2 °C temperature increase and 10 cm depths showing a 1 °C increase.

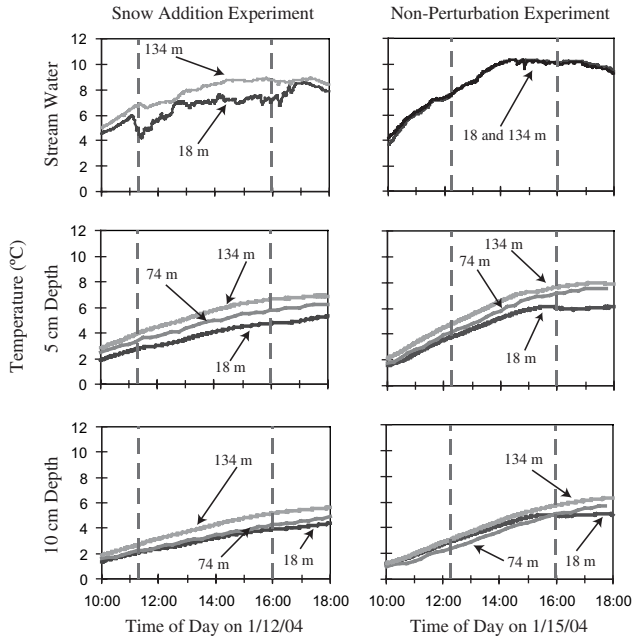


Fig. 10. Streamwater temperatures and 5 and 10 cm-depth streambed temperatures at 18, 74, and 134 m during the two experiments. The dashed lines indicate the start and end of the tracer injections.

In contrast, during the second experiment, stream temperature essentially did not change between the 18 and 134 m sites. The 5 cm hyporheic temperatures did increase 1–2 °C in the reach. The 10 cm hyporheic temperatures cooled slightly by 0.5 °C before warming up 1 °C between the 74 and 134 m sites.

In general, the maximum hyporheic temperatures that were reached by the end of the injections at 16:00, were 0.6–1.4 °C greater during the second experiment than during the snow-addition experiment. However, during the second experiment the starting temperatures were lower and so the overall temperature gain was greater than the maximum values would imply. If starting temperatures at 10:00 are considered, then the temperature gains during the second experiment were 1.3–2.2 °C greater than those in the first.

Table 5 presents changes in streambed temperatures with depth at 18 and 134 m for a representative time period during the non-snow addition experiment. These temperatures are shown alongside representative hyporheic temperatures from other studies. Fig. 11 displays temperatures over the course of the two experiments in both the streambed hyporheic zone and the lateral hyporheic zone at 5 and 10 cm depths and at the frozen boundary. Both Table 5 and Fig. 11 show hyporheic temperatures decreasing with depth. During the two experiments, the hyporheic zone was always cooler than the streamwater.

### 4.8. Reach thermal budgets

The reach heat budgets predicted downstream temperatures at 15-min intervals for the snow addition experiment with an average accuracy of 5.4%. The maximum percent difference between a predicted temperature and an observed temperature was 12.8%. The minimum percent difference was 0.7%. This suggests that the heat balance was a reasonable approximation of heat fluxes in the reach.

In the gaining reach, net radiation accounted for 81.3% of the heat increases while groundwater accounted for 18.6% of the increases (Table 7). However, given the lower hyporheic vs. stream temperatures, the effect of the groundwater gain on the reach's temperature was to cool it by 0.9 °C (Table 6). Net radiation thus accounted for essentially all of the stream warming while groundwater accounted for 39% of stream cooling. In the losing reach, net radiation accounted for essentially all of the heat gains and all of the warming (Tables 6 and 7). Groundwater, in contrast, was responsible for 33% of the heat decreases in the reach (Table 7). Table 6 also shows groundwater loss to be responsible for two percent of the cooling, which does not make sense when considering the physical system. However, there was a five percent difference between the predicted downstream temperature and the observed downstream temperature, and the two percent groundwater cooling may be an artifact of that error. Conduction and hyporheic exchange contribute both to heat loss and stream cooling (Tables 6 and 7).

### 4.9. Cross-sectional thermal budgets

Examination of the cross-sectional thermal budgets as determined for each 15-min interval shows a general trend that as water temperatures increased, evaporation and convection fluxes also increased and that when stream temperatures reached a plateau so did evaporation and convection fluxes. Fig. 12 shows a representative 15-min interval budget for the 143 m location during the snow addition experiment. The other 15-min interval budgets calculated are not presented.

The cross-sectional thermal budgets as averaged for the entire experiment (Table 7) show that during the snow addition experiment, evaporation and convection were the dominant sources of heat loss each accounting for roughly 30% of the losses. Conduction and hyporheic exchange accounted for between 15% and 24% of the heat losses. In contrast, during the second experiment, conduction accounted for 33–38% of the heat losses while evaporation, convection, and hyporheic exchange were responsible for 30%, 24–26%, and 6–13% of the losses respectively. Environmental conditions representative of those used in determining the thermal budgets are presented in Table 8.

Evaporation rates in both the cross-sectional and reach budgets ranged from 2.5 mm $day^{-1}$ at lower water temperatures to 5.0 mm $day^{-1}$ at higher water temperatures. These rates were lower than the 6.2 $mmd^{-1}$ rate determined by Gooseff et al. during a batch pan evaporation experiment in the Lake Hoare basin of Taylor Valley during January 2000 [24].

## 5. Discussion

### 5.1. Comparison of Taylor Valley stream temperatures with those in other regions

Ward [54] reviewed temperature data available for streams in the southern hemisphere and found that equatorial, tropical, and temperate streams had maximum temperatures ranging from 13–30, 22–38, and 6–33 °C, respectively (Table 3). The temperate stream with a maximum temperature of 6 °C was spring-fed. In their review of glacial rivers, Milner and Petts [41] found that summer stream temperatures were generally less than 10 °C. Harper [26] reviewed studies of high latitude streams and reported that mountain desert streams in the Arctic had maximum temperatures ranging from 5–15 °C. Similarly, for eight rivers on the North Slope of Alaska, midday July temperatures ranged from

Table 5
Summer hyporheic temperature patterns

| | | Glacial meltwater stream Switzerland | River Blithe Staffordshire, UK | River Blithe Staffordshire, UK | East branch of Maple River Michigan, USA | Von Guerard Stream (18 m) Taylor Valley, Antarctica | Von Guerard Stream (134 m) Taylor Valley, Antarctica |
|---|---|---|---|---|---|---|---|
| | | Average[a] | Average[b] | Average[b] | Midday | Midday | Midday |
| Surface water temperature (°C) | | 1–6 | 17.8 | 17.8 | 20 | 10.1 | 10.3 |
| $\Delta T$ = change in streambed temperature with depth as compared to surface water temperature (°C) | 5 cm | – | – | – | – | −4.7 | −3.5 |
| | 10 cm | – | – | – | – | −5.8 | −5.6 |
| | 20 cm | ∼0[c] | −1.53 | −4.32 | −7 | −9.7[d] | −7.1 |
| | 30 cm | ∼0 | – | – | – | – | – |
| | 40 cm | – | −2.6 | −4.32 | −11 | – | – |
| Groundwater or frozen boundary temperature (°C) | | N/A | 11.2[e] | 11.2[e] | 8[e] | 0[f] | 0[f] |
| Riparian vegetation | | Sparse, exposed | Rough pasture, exposed | Rough pasture, exposed | Forest | None, exposed | None, exposed |
| Width (m) | | 13 | 4.9 | 4.9 | 7–8 | 2.7 | 2.7 |
| Flow ($m^3 s^{-1}$) | | 7.2 | 0.263 | 0.263 | <0.5 | 0.0004–0.0009 | 0.0004–0.0009 |
| Other site description | | – | Downstream of reservoir; head of riffle | Downstream of reservoir; tail of riffle | Downstream of lake; middle of riffle | Non-snow addition experiment | Non-snow addition experiment |
| Source of information | | [37] | [19] | [19] | [58] | Current study | Current study |

– = Not applicable; N/A = not available.

Data from the snow addition experiment are not presented because the snow addition was used to suppress the midday temperature maximum.

[a] Surface water temperature and 30 cm hyporheic temperature regimes almost identical.

[b] Average daily fluctuation in surface water temperature is 1.8 °C.

[c] Since essentially no temperature change over 30 cm depth, inferring that no temperature change over 20 cm depth.

[d] Temperature change reported is over 23 cm not 20 cm.

[e] Groundwater temperature.

[f] Frozen boundary temperature.

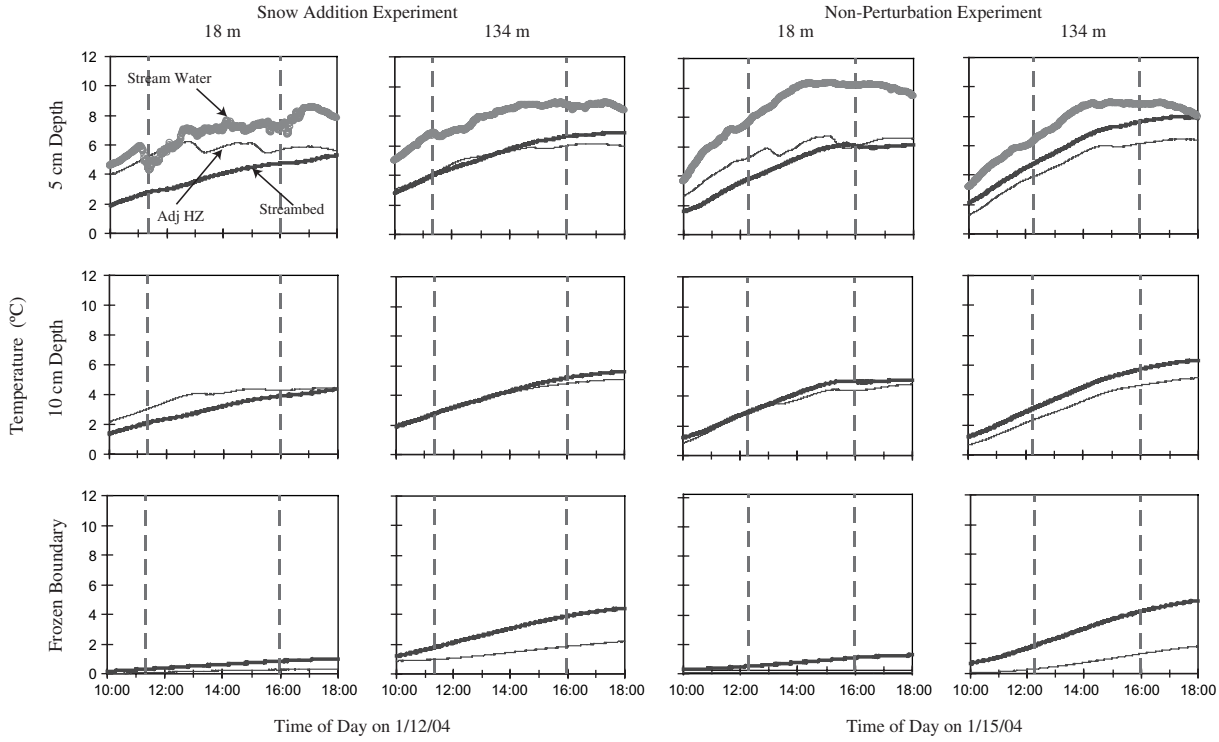


Fig. 11. Streamwater temperatures and streambed and lateral hyporheic zone temperatures during the two experiments at 18 and 134 and at 5, 10 cm, and frozen boundary depths. The thickest continuous line represents streamwater temperatures. The medium-thick continuous line represents streambed temperatures. The thinnest continuous line represents temperatures in the lateral hyporheic zone adjacent to the stream. The dashed lines indicate the start and end of the tracer injections.

Table 6
Reach heat budgets for the snow addition tracer experiment—effects on temperature change

| | Gaining reach | | | Losing reach | | |
|---|---|---|---|---|---|---|
| | °C | % Warming | % Cooling | °C | % Warming | % Cooling |
| $\Delta T_{ws}$, temperature change due to fluxes across the water surface | +2.80 | 100 | – | +3.23 | 100 | – |
| $\Delta T_{gw}$, temperature change due to groundwater inflow or outflow | −0.87 | – | 39.4 | −0.06 | – | 1.8 |
| $\Delta T_{cond}$, temperature change due to conduction | −0.79 | – | 35.9 | −1.37 | – | 55.5 |
| $\Delta T_{hyp}$, temperature change due to hyporheic exchange | −0.54 | – | 24.6 | −1.05 | – | 42.2 |

– = Not applicable.
Friction was negligible.

9.5–15 °C [35]. Also on the North Slope, a beaded tundra stream was found to have temperature maxima of 18–21 °C [29,42]. Beaded streams consists of pools connected by narrow channels. Harper reported that summer temperatures in lowland beaded streams tend to be higher than those of mountain streams [26]. During the 1997–98 summer, Lake Fryxell Basin streams had maximum temperatures ranging from 8 to 15 °C, which were lower than their southern hemisphere equatorial, tropical, and temperate counterparts but comparable to glacial rivers and Arctic streams.

Ward's review [54] also reported annual ranges in stream temperatures and showed them to be generally less than 5 °C, to be 7–15 °C, and to be 0–30 °C for equatorial, tropical, and temperate streams in the southern hemisphere, respectively (Table 3). For the temperate streams, the 0 °C range was for spring-fed streams. Because dry valley streams only flow during the austral summer, the summer season represents the annual range of temperatures. For the 1997–98 summer, Fryxell Basin stream temperatures ranged from 8 to 15 °C. Thus, the annual temperature variation in dry valley streams is comparable to the variation in tropical streams and in many temperate streams.

Finally, Ward found that daily variations in stream temperatures ranged from 0 to greater than 10 °C [54]. Although the minimum daily range was for spring-fed streams, small, heavily-canopied streams also had small daily temperature variations, less than 2–3 °C. Small streams exposed to direct solar radiation and braided

Table 7
Reach and cross-sectional heat budgets for the tracer experiments in W m$^{-2}$

| | Reach budgets (for a particular 15-min interval) | | | | Cross-sectional budgets (averaged over entire experiment) | | | | | | | |
|---|---|---|---|---|---|---|---|---|---|---|---|---|
| | Snow addition experiment | | | | Snow addition experiment | | | | Non-snow addition experiment | | | |
| | Gaining reach | | Losing reach | | 18 m | | 143 m | | 18 m | | 143 m | |
| | (W m$^{-2}$) | % | (W m$^{-2}$) | % | (W m$^{-2}$) | % | (W m$^{-2}$) | % | (W m$^{-2}$) | % | (W m$^{-2}$) | % |
| *Heat gains* | | | | | | | | | | | | |
| Net radiation | 451.2 | 81.3 | 461.1 | 99.9 | 471.1 | 99.9 | 472.8 | 99.9 | 457.7 | 99.99 | 464.8 | 99.99 |
| Friction | 0.6 | 0.1 | 0.6 | 0.1 | 0.6 | 0.1 | 0.4 | 0.1 | 0.1 | 0.01 | 0.1 | 0.01 |
| Condensation | 0 | 0 | 0 | 0 | 0 | 0 | 0 | 0 | 0 | 0 | 0 | 0 |
| Convection | 0 | 0 | 0 | 0 | 0 | 0 | 0 | 0 | 0 | 0 | 0 | 0 |
| Conduction | 0 | 0 | 0 | 0 | 0 | 0 | 0 | 0 | 0 | 0 | 0 | 0 |
| Hyporheic exchange | 0 | 0 | 0 | 0 | 0 | 0 | 0 | 0 | 0 | 0 | 0 | 0 |
| Groundwater | 103.2 | 18.6 | 0 | 0 | – | – | – | – | – | – | – | – |
| *Heat losses* | | | | | | | | | | | | |
| Net radiation | 0 | 0 | 0 | 0 | 0 | 0 | 0 | 0 | 0 | 0 | 0 | 0 |
| Friction | 0 | 0 | 0 | 0 | 0 | 0 | 0 | 0 | 0 | 0 | 0 | 0 |
| Evaporation | 92.9 | 30.0 | 117.69 | 19.4 | 106.8 | 29.8 | 125.4 | 30.5 | 115.1 | 29.1 | 100.3 | 30.7 |
| Convection | 89.3 | 28.8 | 117.44 | 19.4 | 106.4 | 29.7 | 126.0 | 30.6 | 97.8 | 24.8 | 85.3 | 26.1 |
| Conduction | 75.8 | 24.4 | 96.04 | 15.9 | 68.2 | 19.1 | 96.5 | 23.5 | 131.5 | 33.3 | 121.4 | 37.1 |
| Hyporheic exchange | 51.9 | 16.7 | 73.06 | 12.1 | 76.5 | 21.4 | 63.2 | 15.4 | 50.4 | 12.8 | 20.1 | 6.1 |
| Groundwater | 0 | 0 | 200.87 | 33.2 | – | – | – | – | – | – | – | – |

– = Not applicable.

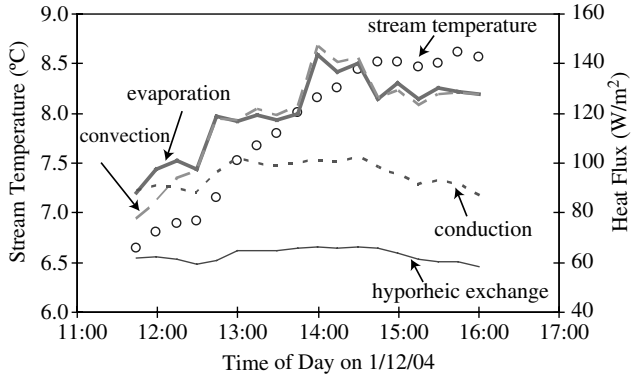


Fig. 12. Cross-sectional thermal budget for the 143 m location during the snow addition experiment. Open circles = water temperature, thin solid line = hyporheic exchange, thick solid line = evaporation, short-dashed line = conduction, long-dashed line = convection. The water temperature scale is on the left *y*-axis and the scale for the heat budget components is on the right *y*-axis.

rivers experienced the maximum daily changes in temperature. With daily temperature changes ranging on average from 6 to 9 °C, Fryxell Basin streams fall in the upper range of daily temperature variation.

### 5.2. Comparison of Taylor Valley hyporheic temperatures with those in other regions

In their review of exchange processes between rivers and groundwater, Brunke and Gonser described general patterns in hyporheic temperatures along an infiltration gradient as decreasing with depth in summer, increasing with depth in winter, and having daily fluctuations that are lagged and attenuated with depth [7]. However, as Brunke and Gonser point out and as will be described in more detail in Section 5.5, in some instances, authors found summer streambed or lateral hyporheic tempera-

Table 8
Environmental conditions during the tracer experiments

| Parameter | Snow addition experiment | | Non-snow addition experiment | |
|---|---|---|---|---|
| | 18 m | 143 m | 18 m | 143 m |
| $H_{radn}$, average net radiation (W m$^{-2}$) | 472.1 | | 461.5 | |
| $U$, average wind speed (m s$^{-1}$) | −1.9 | | −1.7 | |
| $R_h$, average relative humidity | 71.1 | | 55.5 | |
| $T_a$, average air temperature (°C) | −1.9 | | −1.7 | |
| $T_w$, average water temperature (°C) | 6.8 | 7.9 | 9.8 | 8.3 |
| $T_{hyp}$, average hyporheic temperature (°C) | 3.0 | 4.7 | 2.5 | 5.4 |
| $dT_{hyp}/dz$, average streambed temperature gradient (°C m$^{-1}$) | −28.2 | −39.4 | −54.3 | −50.2 |
| $Q$, average discharge rate (L s$^{-1}$) | 7.0 | 7.0 | 0.65 | 0.46 |
| $w$, average stream width (m) | 3.1 | | 2.7 | |

tures to be warmer than associated stream temperatures [37,46,51].

The general decrease in summer hyporheic temperatures can be seen in Table 5, which shows sample hyporheic temperatures from several studies of temperate streams as well as from the non-snow addition experiment. From the table it is evident that hyporheic temperatures vary between surface water and groundwater or frozen boundary temperatures. It is also apparent that attenuation with depth varies among streams, and authors such as Constantz et al. have used temperature profiles to calculate streambed water fluxes [14]. The Swiss glacial meltwater stream represents one end of the spectrum in which stream temperatures show essentially no attenuation at a 30 cm depth while hyporheic temperatures in the Michigan stream and in Von Guerard Stream show much stronger attenuation and thus higher thermal gradients at a 20 cm depth. In the case of Von Guerard Stream, these comparatively strong gradients may reflect the influence of the frozen boundary, which was only about 20 cm below the streambed surface during the experiments.

### 5.3. Sources of uncertainty in the heat budgets

One goal of our study was to obtain an overview of the importance of various heat budget terms in dry valley streams. In establishing the budgets, several sources of uncertainty became apparent. The lack of micrometeorological data for the experimental reach is one such source. Johnson points out that environmental gradients can vary over just short distances away from streams [30], and Brown notes that for small streams, with their lower capacity for heat storage, it is necessary to be more precise when defining the heat budget in order to obtain a given level of accuracy in temperature prediction [6]. Because the experimental reach was located in an open area with no terrestrial vegetation to introduce shading or block the wind, these spatial variations may not be as pronounced in the Dry Valleys.

The use of a dual tracer injection approach and analysis with the OTIS-P transient storage model reduced uncertainty in the terms related to flow and hyporheic exchange. However, the streambed temperature profiles used in the heat budgets present a greater source of error. We represented temperatures in the hyporheic zone ($T_{hyp}$) and the thermal gradients in the hyporheic zone ($dT/dz$) with average values. Yet as Story et al. mention, there can be substantial spatial variability in streambed temperature gradients [50]. The temperature gradients in the experimental reach are non-linear, making the decision of what $T_{hyp}$ and $dT/dz$ values to use more complicated.

Finally the stream systems in the Dry Valleys are underlain by permafrost with an active layer that thaws and freezes throughout the summer. Our thermal budgets did not include a heat term associated with phase changes at a frozen boundary.

### 5.4. Processes and factors influencing streamwater warming: radiation patterns, playa regions

All the Fryxell Basin streams whose temperature patterns were analyzed exhibited pronounced coincident diel cycles in temperature (Fig. 3). Similarly, except for the uppermost site, the sites along the 5-km length of Von Guerard Stream exhibited pronounced diel cycles with simultaneous temperature peaks (Fig. 4). The diel cycles observed in both datasets closely mimicked the diel patterns in net shortwave radiation. The simultaneous diel temperature peaks along Von Guerard Stream agree with findings presented by Constantz et al. for a mountain stream and a desert stream in the western United States [12]. However, they contrast with the findings of Smith that indicated that peak stream temperatures were delayed with distance downstream [47,48].

The cross-sectional thermal budget calculations show why stream warming in the Lake Fryxell Basin and net shortwave radiation patterns are so closely matched. Net radiation accounted for 99.9% of the heat gained by the stream. This contrasts with streams studied by Webb and Zhang in Devon England [57]. In Devon, convection played a greater role in warming the streams during the summer because, unlike in the Dry Valleys, air temperatures were greater than water temperatures. In winter, conduction contributed heat to the Devon streams because streambed temperatures were greater than water temperatures. During high flow periods, heat added to the streams from fluid friction was also significant.

Dry valley streams experience higher flow periods as well with flow varying greatly on daily, seasonal, and interannual timescales [10]. While flows in Von Guerard Stream during the experiments were quite low, on the order of 0.5–6 L/s, during other years Von Guerard flows have reached values of 400 L/s, and flows in other Lake Fryxell Basin streams have on occasion reached values of 900 L/s. During such times, friction could play a greater role in warming dry valley streams, in particular in the more steep upper reaches.

Another factor explaining the coincidence of the temperature and net shortwave radiation peaks is the shallowness of Fryxell Basin streams, typically less than 0.3 m. Vugts reported the rapid response of a small stream to meteorological conditions [53], and a study by Clark et al. showed that water in shallow areas along the channel margins reached maximum and minimum daily temperatures an average of 180 and 100 min earlier, respectively, than water in the main channel [9]. Shallow depths may play a role in localized areas of heat gain in Von Guerard Stream. The large playa region

where the depth is only a few centimeters is an area in which a 3–6 °C warming of streamwater took place.

Although we found that hyporheic exchange cooled the stream at midday, at other times of day, it is possible that hyporheic exchange might warm the stream. Johnson proposed that this might be the case for nighttime hyporheic flow [31]. A study by Webb and Zhang [56] found that that streams in Dorset, UK experienced a diel cycle in bed conduction with conduction acting as a heat source to the stream at nighttime and a heat sink during the day. The warmer streambed temperatures at night, compared to stream temperatures would suggest that, as with conduction, hyporheic exchange might warm the stream at night.

In addition, our longitudinal study of temperatures in Von Guerard Stream showed downstream warming suggesting that dry valley streams might experience upstream/downstream differences in the influence of hyporheic exchange. Milner and Petts [41] found that meltwater close to the glacier snout was near 0 °C but that temperatures showed marked diel variation that typically increased downstream. In cooler upstream sections of dry valley streams, hyporheic temperatures might be greater than those in the stream and thus hyporheic exchange might result in stream warming. Others have found summer streambed or lateral hyporheic zone temperatures to be higher than associated stream temperatures, for instance in a glacial stream in the Swiss Alps, in a stream in British Columbia, and in a southwest US desert stream, and have attributed the warmer temperatures to flow through exposed areas of the riverbed [37,46,51].

### 5.5. Processes cooling streamwater temperatures: snowfields, evaporation, convection, conduction, and hyporheic exchange

Although the McMurdo Dry Valleys are a polar desert ecosystem that receive on average less than 10 cm water equivalent of precipitation each year in the form of snow [5], the snow that falls often collects in patches along the stream channels when redistributed by winds. Longitudinal variations in water temperatures in Von Guerard Stream indicate that upstream snowfields cool the stream. Temperature results from the snow addition tracer experiment provide direct experimental evidence that contact with snow during flow through a snowfield can significantly cool stream temperatures, e.g. by 1–2 °C in a short stream reach. Thus, despite the low amounts of snowfall, snow may play a significant role in modifying the temperatures of Von Guerard Stream. Snow likely modifies the temperatures in other dry valley streams as well. The role played by snow will depend on the distribution of snow patches along the stream length and on the persistence of those patches, which in turn will depend on their size and location within the valleys and on meteorological conditions. Gooseff et al. [23] presented data showing that during one summer, three of four snow patches located along lakeshores in the Dry Valleys disappeared completely. This suggests that the influence of snow on stream temperatures may be greater earlier in the summer before snow melts entirely.

Another process that can cool dry valley streams is hyporheic exchange. Throughout both tracer experiments, hyporheic temperatures were colder than instream temperatures. Thus, the hyporheic zone represents a reservoir of cooler water that is hydrologically connected to the main channel and cools the stream through active exchange processes.

The tracer experiments provide direct evidence of such cooling taking place in the most downstream segment of the experimental reach. In both experiments chloride concentrations decreased between the 134 and 143 m sites, indicating that the stream was gaining water. The streamwater temperatures also decreased by 0.5–1.5 °C in this reach in both experiments. The water gained must have come from the hyporheic zone, and because the reach was so short, there was little opportunity for instream warming to take place and mask the cooling. Analysis of streambed monitoring well samples showed that chloride concentrations in the wells matched or slightly exceeded instream concentrations. Hyporheic water coming from the streambed would thus not have diluted the instream concentrations. This suggests that hyporheic water coming from areas adjacent to the stream was responsible for the dilution and cooling. Through analysis of changes in the isotopic signature of streamwater over several weeks at the initiation of flow, Gooseff et al. [24] showed that water in this lateral hyporheic zone interacted with the stream, and was a source of solutes to the stream.

The cross-sectional thermal budgets for the tracer injection experiments quantify the influence of hyporheic exchange on the heat flux in streams and allow comparison with the influence of evaporation, convection, and conduction. During the snow addition experiment, evaporation and convection were the dominant sources of heat loss while during the second experiment conduction was responsible for the greatest loss. This difference reflects the differing environmental conditions during the experiments. During the snow addition experiment, stream temperatures were cooler and the thermal gradients between the stream and streambed were less, reducing conduction. Hyporheic exchange played a much greater role in cooling the stream in the snow addition experiment than it did during the second experiment. Although the exchange coefficients were similar for both experiments (Table 4), the hyporheic zone cross-sectional area, $A_s$, during the snow-addition was nearly three times that of the second experiment, enhancing the cooling effect of hyporheic exchange. This difference in $A_s$ might be attributed to the drastically different

flows during the two experiments (Fig. 8). The differing degrees of hyporheic exchange may also have contributed to the differences in conduction because the exchange of water between the stream and the hyporheic zone will reduce the streambed temperature gradient. The greater hyporheic exchange contribution during the snow addition experiment coincided with a smaller contribution from conduction.

The cross-sectional thermal budgets can be compared in a qualitative way with the budgets established by Webb and Zhang for study reaches in four streams in Devon, England [57]. Webb and Zhang found that convection added heat to the streams during the summer and removed it during the winter. In contrast, conduction acted as a heat sink during the summer and a heat source during the winter. Evaporation was a consistent source of heat loss throughout the year. With water temperatures that, in particular at midday, can be warmer than both air and hyporheic temperatures, dry valley streams experience winter-like convection and summer-like conduction. So, in contrast to their Devon counterparts, convection and conduction work in conjunction to cool the streams in addition to evaporation and hyporheic exchange. Thus although dry valley streams are exposed directly to the warming influence of solar radiation, a combination of cooling processes restrict maximum stream temperatures.

The gaining reach thermal budget for the snow addition experiment presented in terms of temperature change (Table 6) can be compared with that constructed by Story et al. for a gaining stream reach in British Columbia, Canada [50]. Both budgets were constructed for midday time periods. The British Columbia stream reach was an average 1.3–1.4 m in width and was shaded by a forest canopy in contrast to the average 3.1 m width and exposed nature of Von Guerard Stream. The thermal budgets for the two streams were generally similar. Heat fluxes at the water surface accounted for all heat gains in both budgets. Groundwater, conduction, and hyporheic exchange accounted for 41%, 35%, and 24% of the cooling in the British Columbia stream, respectively, and for 39%, 36%, and 25% of the cooling in Von Guerard Stream, respectively. In the thermal budget for the losing reach condition, both conduction and hyporheic exchange played a much greater role in cooling the stream, accounting for 56 and 42% of the cooling respectively (Table 6).

### 5.6. Constraints on stream temperature maxima

Data from the temperature profile along Von Guerard Stream show that in certain reaches little temperature change occurs. The temperatures in these reaches appear to converge on a similar value for a given day (Fig. 4). Similarly, data for seven streams in the Lake Fryxell Basin also show that temperatures in the five warmest streams, Aiken, Delta, Green, Lost Seal, and Von Guerard, converged on a similar value for a given day despite having lengths that varied widely from 1.2 to 11.2 km (Fig. 3, Table 1) [10]. These lines of evidence suggest that at a certain point in situ stream warming by solar radiation is balanced by the cooling processes identified in the thermal budgets. The results displayed on Fig. 12 suggest that evaporation and convection in particular may constrain stream temperature maxima. As stream temperature increased so did the magnitude of evaporation and convection. In our analysis, the hyporheic exchange rate and hyporheic storage area were held constant. However, hyporheic exchange rates might rise with increasing stream temperatures. In some streams, a decrease in viscosity with increasing temperature has been connected to increased infiltration [12]. It may be that as stream temperatures increase, infiltration increases, enhancing the mixing of streamwater with cooler hyporheic zone water, which would, in turn, counteract solar warming.

Another constraint on temperature maxima in dry valley streams may be the magnitude of streamflows at the time the radiation maxima occur. Conovitz et al. [10] showed that diel peaks in streamflow occur some time after the sun shines directly on the vertical face of the source glacier, and flows in different streams peak at different times of day. Flows in Canada Stream, for instance, reach daily maxima between 14:30 and 16:00, which is when stream temperatures tend to peak. Consequently, in Canada Stream a given intensity of solar radiation must warm a greater volume of water than in other streams that have later peak flows. This could explain the lower temperature maxima observed in Canada Stream. The fact that, at 1.5 km, Canada Stream is one of the shorter streams in the valleys (Table 1) may also play a role in that Canada Stream water may not have as much travel time to warm as water in other streams. However, as noted, several other streams in the Fryxell basin with lengths ranging from 1.2 to 11.2 km warmed to a similar degree.

Finally, flow regimes may also constrain stream temperature maxima by affecting the influence of hyporheic exchange. Johnson noted that the magnitude of hyporheic influence is related to the proportion of streamwater flowing through the hyporheic zone [31]. At low flows in the Dry Valleys, this proportion may be greater than 50% [11]. Thus, in the experimental reach, this might result in lower stream temperature maxima at lower discharges and higher stream temperature maxima at intermediate discharges. At higher discharges, stream temperature maxima may again be lower because of the thermal inertia of water.

### 5.7. Hyporheic exchange warms the hyporheic zone and erodes the frozen boundary

During both experiments, the streamwater was always warmer than the hyporheic water. Thus, any mixing of

streamwater with hyporheic water would increase hyporheic temperatures. During both experiments hyporheic temperatures at 5 and 10 cm depths at 134 m were 1–2 °C warmer than those at the 18 m site (Fig. 10). Chloride monitoring well data for both experiments showed a stronger hyporheic-stream connection at 134 m than at 18 m (Fig. 9). In combination, these results suggest that greater hyporheic exchange resulted in warmer hyporheic temperatures.

A comparison of results from the snow addition experiment with those from the non-perturbation experiment shows that the snow addition resulted in stream temperatures that were 1.5–3 °C cooler than those during the second set of injections. The maximum hyporheic temperatures reached at 5 and 10 cm depths reached during the snow addition were also cooler, by 0.6–1.4 °C, than those attained during the second experiment. The total amount of warming that took place from 10:00 to 16:00 during the first experiment was also less, by 1.3–2.2 °C, than that during the non-perturbation injections.

During the two experiments, several lines of evidence show that significant hyporheic exchange occurred. These include: rising chloride concentrations in streambed wells, the large 60–70 μS/cm increase in specific conductance between 18 and 134 m, and the dispersion of the injected chloride pulse. In addition, the long travel times in the second experiment are indicative of exchange. In conjunction, the temperature data and hyporheic exchange evidence suggest that the difference in streamwater temperatures between the two days was transmitted via hyporheic exchange to the hyporheic zone so that different stream temperatures led to different degrees of hyporheic warming. However, the interpretation of the data is complicated by the differing flow regimes during the two experiments.

During the snow addition injections the reach switched between gaining and losing while during the second experiment the reach consistently lost water. Since water was flowing from the hyporheic zone into the stream during part of the snow addition experiment, this and not solely the difference in stream temperatures between the two experiments could account for the decreased hyporheic temperature gain observed. Likewise, the consistent loss of water from the stream to the hyporheic zone during the non-perturbation experiment could have contributed to the increased hyporheic temperature gain observed when compared to that of the snow addition experiment.

As well as indicating that hyporheic exchange warmed the hyporheic zone, the results of the tracer experiments indicate that the infiltration of warmer streamwater affected the frozen boundary. During both experiments temperatures at the frozen boundary showed a 1 °C increase at the 18 m site and a 3–4 °C increase at the 134 m site. The deeper monitoring well at the 134 m site was screened at a depth of 9–19 cm, close to the 20 cm deep frozen boundary. The chloride data from this well indicate that streamwater reached the frozen boundary. Although the deeper monitoring well at the 18 m site was screened at a depth of 7–17 cm, six cm above the 23 cm deep frozen boundary, chloride data also indicate that streamwater approached the frozen boundary.

Overall these results suggest that advection of warmer streamwater into the hyporheic zone erodes the frozen boundary, expanding the hyporheic zone during the summer. This would be important at the watershed scale because the hyporheic zone influences hydrologic, biogeochemical, and ecological processes in the streams.

### 5.8. Streams as vectors of heat in the valleys

Not only do the streams transport warm water downstream and carry heat into the hyporheic zone, eroding the frozen boundary, streams in the Fryxell Basin transport warm water into the lake on the valley floor. The seven streams whose temperatures were analyzed have simultaneous temperature peaks. It is reasonable to assume that temperatures in the remaining three streams, given their flow paths and source glaciers, also peak at similar times of day. This finding indicates that a pulse of warm water, or a thermal wave, enters Lake Fryxell once a day, coming predominantly from the south and east sides of the basin. Because of Lake Fryxell's permanent, 4-m thick ice cover, solar radiation is greatly attenuated before reaching the water column, except in the moats that develop along the outside edges of the lake during the summer. Warm streamwater may directly enter the lake under the ice-cover or may mix with moat water, depending on the extent of the moat. Streams may thus comprise an important source of heat influencing the thermal processes and circulation of the lakes.

## Acknowledgements

We thank Beth Bartel, Justus Brevik, Bija Sass, Zondra Skertich, Rae Spain, Kathy Welch, and especially Christopher Jaros and Justin Joslin for their help in the field. Valuable logistical support was provided by Tracey Baldwin, Jessie Crain, and Howard Tobin of Raytheon Polar Services and by PHI Helicopters Inc. We thank Rich Wanty of the USGS Denver Federal Center for analytical assistance and Rob Runkel for help with the OTIS-P modeling. The authors also appreciate the comments provided by Arne Bomblies, Gary Clow, Sabre Duren, Greg Pasternack, and four anonymous reviewers on the manuscript. This work was supported by NSF project OPP-9810219.

## References


[1] Alger AS, McKnight DM, Spaulding SA, Tate CM, Shupe GH, Welch KA, Edwards R, Andrews ED, House HR. Ecological processes in a cold desert ecosystem: the abundance and species of algal mats in glacial meltwater streams in Taylor Valley, Antarctica. Institute of Arctic and Alpine Research, Boulder, CO-Occasional Paper 51, 1997. 108 p.

[2] Allan JD. Stream ecology—structure and function of running waters. Boston: Kluwer Academic Publishers; 2000.

[3] Bencala KE. Hyporheic zone hydrological processes—invited commentary. Hydrol Process 2000;14:2797–8.

[4] Bomblies A, McKnight DM, Andrews ED. Retrospective simulation of lake level rise in Lake Bonney based on recent 21-year record: indication of recent climate change in the McMurdo Dry Valleys. J Paleolimnol 2001;25:477–92.

[5] Bromley AM. Weather observations, Wright Valley, Antarctica. New Zealand Meteorological Service, Wellington—Publ 11, 1985. 37 pp.

[6] Brown GW. Predicting temperatures of small streams. Water Resour Res 1969;5(1):68–75.

[7] Brunke M, Gonser T. The ecological significance of exchange processes between rivers and groundwater. Freshwater Biol 1997;37:1–33.

[8] Chapra SC. Surface water-quality modeling. Boston: McGraw-Hill; 1997.

[9] Clark E, Webb BW, Ladle M. Microthermal gradients and ecological implications in Dorset rivers. Hydrol Process 1999;13: 423–38.

[10] Conovitz PA, McKnight DM, MacDonald LH, Fountain AG, House HR. Hydrologic processes influencing streamflow variation in Fryxell Basin, Antarctica. Ecosystem dynamics in a polar desert: The McMurdo Dry Valleys. Washington, DC: American Geophysical Union; 1998. p. 93–108.

[11] Conovitz P. Active layer dynamics and hyporheic zone storage in three streams in the McMurdo Dry Valleys, Antarctica, M.S. Thesis, Colorado State University, USA, 2000.

[12] Constantz J, Thomas CL, Zellweger G. Influence of diurnal variations in stream temperature on streamflow loss and groundwater recharge. Water Resour Res 1994;30(12):3253–64.

[13] Constantz J. Interaction between stream temperature, streamflow, and groundwater exchanges in alpine streams. Water Resour Res 1998;34(7):1609–15.

[14] Constantz J, Stewart AE, Niswonger R, Sarma L. Analysis of temperature profiles for investigating stream losses beneath ephemeral channels. Water Resour Res 2002;38(12). Art. No. 1316.

[15] Dana GL, Wharton RA. Solar radiation in the McMurdo Dry Valleys, Antarctica. In: Dynamics in a polar desert: The McMurdo Dry Valleys. Washington, DC: American Geophysical Union; 1998. p. 39–64.

[16] Dingman SL. Physical hydrology. 2nd ed. Upper Saddle River, New Jersey: Prentice Hall; 2002.

[17] Doran PT, Wharton RA, Lyons WB. Paleolimnology of the McMurdo Dry Valleys, Antarctica. J Paleolimnol 1994;10:85–114.

[18] Doran PT, McKay CP, Clow GD, Dana GL, Fountain AG, Nylen T, Lyons WB. Valley floor climate observations from the McMurdo Dry Valleys, Antarctica, 1986–2000. J Geophys Res 2002;107(D24). Art. No. 4772.

[19] Evans EC, Petts GE. Hyporheic temperature patterns within riffles. Hydrol Sci J 1997;42(2):199–213.

[20] Findlay S. Importance of surface–subsurface exchange in stream ecosystems: the hyporheic zone. Limnol Oceanogr 1995;40: 159–64.

[21] Fountain AG, Lyons B, Burkins MB, Dana GL, Doran PT, Lewis KJ, McKnight DM, Moorhead DL, Parsons AN, Priscu JC, Wall DH, Wharton Jr RA, Virginia RA. Physical controls on the Taylor Valley Ecosystem, Antarctica. BioScience 1999;49(12): 961–71.

[22] Gooseff MN, McKnight DM, Lyons WB, Blum AE. Weathering reactions and hyporheic exchange controls on streamwater chemistry in a glacial meltwater stream in the McMurdo Dry Valleys. Water Resour Res 2002;38(12).

[23] Gooseff MN, Barrett JE, Doran PT, Fountain AG, Lyons WB, Parsons AN, Porazinska DL, Virginia RA, Wall DH. Snow-patch influence on soil biogeochemical processes and invertebrate distribution in the McMurdo Dry Valleys, Antarctica. Arctic, Antarctic, and Alpine Research 2003;33(1):91–9.

[24] Gooseff MN, McKnight DM, Runkel RL, Vaughn BH. Determining long time-scale hyporheic zone flow paths in Antarctic streams. Hydrol Process 2003;17:1691–710.

[25] Gooseff MN, McKnight DM, Runkel RL, Duff JH. Denitrification and hydrologic transient storage in a glacial meltwater stream, McMurdo Dry Valleys, Antarctica. Limnol Oceanogr 2004;49(5):1884–95.

[26] Harper PP. Ecology of streams at high latitudes. In: Lock MA, Williams DD, editors. Perspectives in running water ecology. New York: Plenum Press; 1981. p. 313–37.

[27] Hendy CH, Healy TR, Raymer EM, Shaw J, Wilson AT. Late Pleistocene glacial chronology of the Taylor Valley, Antarctica and the global climate. Quat Res 1979;11:172–84.

[28] Howard-Williams C, Vincent CL, Broady PA, Vincent WF. Antarctic stream ecosystems: variability in environmental properties and algal community structure. Internationale Revue der gesamten Hydrobiolgie 1986;71:511–44.

[29] Irons III JG, Oswood MW. Seasonal temperature patterns in an arctic and two subarctic Alaskan (USA) headwater streams. Hydrobiologia 1992;237:147–57.

[30] Johnson SL. Stream temperature: scaling of observations and issues for modeling. Hydrol Process 2003;17:497–9.

[31] Johnson SL. Factors influencing stream temperature in small streams: substrate effects and a shading experiment. Can J Fish Aquat Sci 2004;61:913–23.

[32] Lapham WW. Use of temperature profiles beneath streams to determine rates of vertical ground water flow and vertical ground water conductivity. US Geological Survey Water Supply Paper 2337, 35. 1989.

[33] Keys JR. Air temperature, wind, precipitation, and atmospheric humidity in the McMurdo Region. Geology Department, Victoria University, Wellington, New Zealand—Publ 17, 1980. 57 p.

[34] Kilpatrick F, Cobb E. Measurement of discharge using tracers. Techniques of water-resources investigations of the United States Geological Survey. Book 3—Applications of hydraulics, Chapter A16, 1985.

[35] Kling GW, O'Brien WJ, Miller MC, Hershey AE. The biogeochemistry and zoogeography of lakes and rivers in arctic Alaska. Hydrobiologia 1992;240:1–14.

[36] Lyons WB, Welch KA, Neumann K, Toxey JK, McArthur R, Williams C, McKnight DM, Moorhead D. Geochemical linkages among glaciers, streams, and lakes within Taylor Valley, Antarctica. Ecosystem dynamics in a polar desert: The McMurdo Dry Valleys. Washington, DC: American Geophysical Union; 1998. p. 77–92.

[37] Malard F, Mangin A, Uehlinger U, Ward JV. Thermal heterogeneity in the hyporheic zone of a glacial floodplain. Can J Fish Aquat Sci 2001;58:1319–35.

[38] McKnight DM, Alger A, Tate CM. Longitudinal patterns in algal abundance and species distribution in meltwater streams in Taylor Valley, Southern Victoria Land, Antarctica. In: Ecosystem dynamics in a polar desert: The McMurdo Dry Valleys. Washington, DC: American Geophysical Union; 1998. p. 93–108.

[39] McKnight DM, Niyogi DK, Alger AS, Bomblies A, Conovitz PA, Tate CM. Dry valley streams in Antarctica: ecosystems waiting for water. BioScience 1999;49(12):985–95.
[40] McKnight DM, Runkel RL, Tate CM, Duff JH, Moorhead D. Inorganic nitrogen and phosphorus dynamics of Antarctic glacial meltwater streams as controlled by hyporheic exchange and benthic autotrophic communities. J North Am Benthol Soc 2004;23:171–88.
[41] Milner AM, Petts GE. Glacial rivers: physical habitat and ecology. Freshwater Biol 1994;32:295–307.
[42] Oswood MW, Everett KR, Schell DM. Some physical and chemical characteristics of an arctic beaded stream. Holarctic Ecol 1989;12:290–5.
[43] Péwé TL. Multiple glaciation in the McMurdo Sound Region, Antarctica—a progress report. J Geol 1960;68:498–514.
[44] Poole GC, Berman CH. An ecological perspective on in-stream temperature: natural heat dynamics and mechanisms of human-caused thermal degradation. Environ Manage 2001;27(6): 787–802.
[45] Runkel RL, McKnight DM, Andrews ED. Analysis of transient storage subject to unsteady flow: diel flow variation in an Antarctic stream. J North Am Benthol Soc 1998;17(2):143–54.
[46] Shepherd BG, Hartman GF, Wilson WJ. Relationships between stream and intergravel temperatures in coastal drainages, and some implications for fisheries workers. Can J Fish Aquat Sci 1986;43:1818–22.
[47] Smith K. Some thermal characteristics of two rivers in the Pennine area of northern England. J Hydrol 1968;6:405–16.
[48] Smith K. River water temperatures—an environmental review. Scott Geograph Mag 1972;88:211–20.
[49] Stanford JA, Ward JV. An ecosystem perspective of alluvial rivers: connectivity and the hyporheic corridor. J North Am Benthol Soc 1992;12:48–60.
[50] Story A, Moore RD, Macdonald JS. Stream temperatures in two shaded reaches below cutblocks and logging roads: downstream cooling linked to subsurface hydrology. Can J For Res 2003;33:1383–96.
[51] Valett HM, Fisher SG, Stanley EH. Physical and chemical characteristics of the hyporheic zone of a Sonoran Desert stream. J North Am Benthol Soc 1990;9:201–15.
[52] Von Guerard P, McKnight DM, Harnish RA, Gartner JW, Andrews ED. Streamflow, water-temperature, and specific-conductance data for selected streams draining into Lake Fryxell, Lower Taylor Valley, Victoria Land, Antarctica, 1990–92. US Geological Survey Open-File Report 94-545, 1995.
[53] Vugts HF. Calculation of temperature variations of small mountain streams. J Hydrol 1974;23:267–78.
[54] Ward JV. Thermal characteristics of running waters. Hydrobiologia 1985;125:31–46.
[55] Webb BW, Zhang Y. Spatial and seasonal variability in the components of the river heat budget. Hydrol Process 1997;11: 79–101.
[56] Webb BW, Zhang Y. Water temperatures and heat budgets in Dorset chalk water courses. Hydrol Process 1999;13:309–21.
[57] Webb BW, Zhang Y. Intra-annual variability in the non-advective heat energy budget of Devon streams and rivers. Hydrol Process 2004;18:2117–46.
[58] White DS, Elzinga CH, Hendricks SP. Temperature patterns within the hyporheic zone of a northern Michigan river. J North Am Benthol Soc 1987;6(2):85–91.